Mathematical Biosciences and Engineering

https://www.aimspress.com/journal/mbe

MBE, 21(3): 3999–4035.
DOI: 10.3934/mbe.2024177
Received: 18 December 2023
Revised: 30 January 2024
Accepted: 04 February 2024
Published: 22 February 2024

Research article

Sexually transmitted infections and dating app use

Carlos Bustamante Orellana[1], Jordan Lyerla[2], Aaron Martin[1] and Fabio Milner[1,*]

[1] Simon A. Levin Mathematical, Computational and Modeling Sciences Center, Arizona State University, Engineering Center, A Wing, AZ 85287-3901, USA

[2] Department of Biology, Univeristy of Kansas, 1200 Sunnyside Ave., Lawrence, KS 66045, USA

* **Correspondence:** Email: milner@asu.edu; Tel: +1-480-727-2691; Fax: +1-480-727-7346.

Abstract: Incidence of sexually transmitted infections (STIs) is rising sharply in the United States. Between 2014 and 2019, incidence among men and women has increased by 62.8% and 21.4%, respectively, with an estimated 68 million Americans contracting an STI in 2018.[a] Some human behaviors impacting the expanding STI epidemic are unprotected sex and multiple sexual partners.[b] Increasing dating app usage has been postulated as a driver for increases in the numbers of people engaging in these behaviors. Using the proposed model, it is estimated that both STI incidence and prevalence for females and males have increased annually by 9%–15% between 2015 and 2019 due to dating apps usage, and that STI incidence and prevalence will continue to increase in the future. The model is also used to assess the possible benefit of in-app prevention campaigns.

[a] https://www.cdc.gov/nchhstp/newsroom/ fact-sheets/std/STI-Incidence-Prevalence-Cost-Factsheet.htm

[b] A. N. Sawyer, E. R. Smith, and E. G. Benotsch. Dating application use and sexual risk behavior among young adults. Sexuality Research and Social Policy, 15:183–191, 2018.

Keywords: STIs; two-sex epidemic models; phone dating apps; contact rates

1. Introduction

Sexually transmitted infections (STIs), also referred to as sexually transmitted diseases (STDs), are very widespread in the U.S. and cause many short- and long-term health problems, as well as incur great expenses to treat them. The Centers for Disease Control and Prevention's (CDC) latest estimates indicate that 68 million people (20% of the U.S. population or approximately one in five people) had an STI on any given day in 2018, with 25 million of them newly acquired that year, and these cost the American healthcare system nearly $16 billion in direct medical costs alone [1].

The eight most common sexually transmitted infections (STIs) are chlamydia, gonorrhea, syphilis,

trichomoniasis, hepatitis B virus (HBV), herpes simplex virus type 2 (HSV-2), human immunodeficiency virus (HIV), and human papillomavirus (HPV). The first three are caused by bacteria, and the fourth by protozoa, and they are generally curable with existing single-dose regimens of antibiotics lasting 1-4 weeks. The last four are viral infections. For the first three of these, the best available treatments are antivirals, while for HPV, there is no direct treatment, but preventive vaccines are available [2]. Table 1 summarizes their nationwide prevalence and incidence in 2018 [1].

Table 1. Prevalence and incidence of the 8 most common STIs, U.S. 2018.

STI	Prevalence (in millions)	Incidence (in millions)
Chlamydia	2.4	4
Gonorrhea	0.209	1.6
Syphilis	0.156	0.146
Trichomoniasis	2.6	6.9
HBV	0.103	0.0083
HSV-2	18.6	0.572
HIV	0.984	0.0326
HPV	42.5	13

One recent social change that has been postulated to modify human sexual behavior, and in turn the incidence and prevalence of STIs, is the advent of dating apps. For context, mobile phone and dating website applications have seen a global surge in usage since the start of COVID-19. For example, in the first quarter of 2022, 39% of all single, divorced, or widowed consumers reported use of an online dating site in the previous month [3]. This trend in human dating behavior is consistent with the recorded 17 million daily users among the top twenty dating apps in 2020 [4]. This data is further corroborated by statistics that state 26.6 million Americans used a smartphone dating app in 2020, with Tinder reporting 957,700 downloads in the month of June 2022 alone [5].

Researchers from The Chicago School of Professional Psychology found a relationship between sexual discounting, usage of dating applications, and sexual risk. Delay discounting refers to the devaluation of an objective as a function of increasing time; correspondingly, sexual discounting indicates the devaluation of protected sex in favor of unprotected, immediate sex. The researchers utilized Kendall's τ-b to calculate the correlation between risky sexual behavior and sexual discounting for dating app users and non-users. Their results give evidence of a strong correlation among users ($r = -0.357$) and no correlation among dating app non-users ($r = -0.05$). This adds support to the hypothesis that dating apps may play a significant role in increasing STI rates [6].

The relationship between risky sexual behavior and dating app usage is significant as such behaviors have been linked to increased STI infection rates. Several critical risky sexual behaviors have been associated with dating app use: unprotected sex, multiple sexual partners, sex after too much to drink, and sex after using drugs. In a 2017-study to evaluate the correlation between these sexual risk behaviors and dating app usage, the authors surveyed 509 heterosexual, cisgender undergraduate students (18-25 years old) from a psychology class at a Mid-Atlantic institution. The survey evaluated the students' impulsivity, dating app usage and motivations, sexual behavior, and demographics. It was found that individuals who seek sexual partners through dating websites and apps have higher rates of unprotected sex, higher rates of STIs, and a greater number of sexual partners; the individuals who

used dating apps were also found to be more impulsive [7] compared with those who did not use the apps.

STI incidence is heteregeneous across age and sex. As an example of age heterogeneity, we present in Figure 1 the age probability density function for newly infected females for chlamydia [8]. It follows approximately a gamma distribution plotted in blue as $f(a) = 5.35\ \gamma(a, 9.2, 1.95)$. They hit particularly hard the younger population of 15-to-24-year-olds [9].

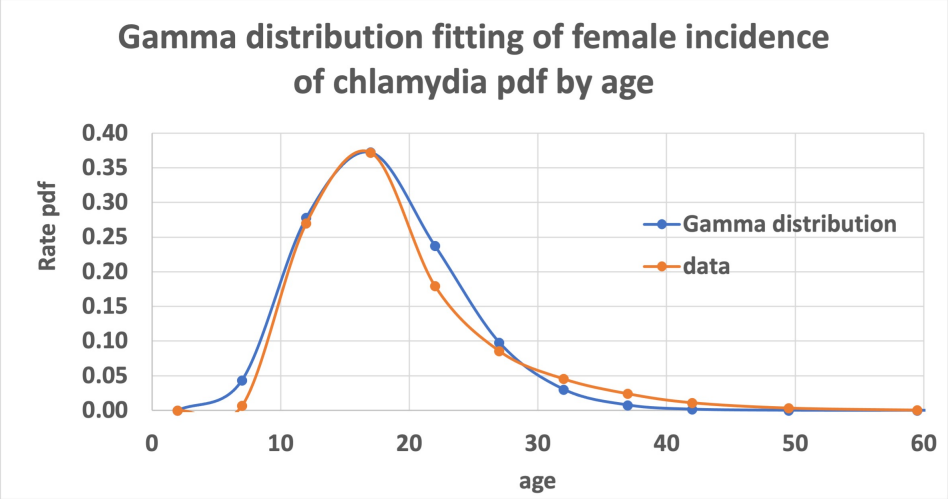

Figure 1. Age probability density function for incidence of chlamydia among females.

The extant literature presents a qualitative correlation between dating app usage, sexual risk behavior, and STIs, but fails to provide a quantitative assessment of the impact dating apps have on increasing STI incidence. As such, this study attempts to use SIS epidemic modeling in order to quantify the increase in STIs that has resulted from the use of dating apps. In order to use our SIS models, several types of data are needed to estimate model parameters. We found a scarcity or absence of such data.

To combat the rising STI rates, prevention campaigns within dating apps have been proposed as a possibility. In one study the authors performed in-depth interviews of 25 men who have sex with men to qualitatively assess the potential to deliver sexual health information and promotion through dating apps. Results indicate that these interventions are acceptable and have the potential to reduce STI rates. We will use our models to provide a quantitative assessment of the possible impact that this study suggests, so as to quantify the reduction of STI incidence that dating apps' prevention campaigns may induce [10].

In summary, the four main objectives of the present study are: 1) to introduce a two-sex model of STIs with same-sex and opposite-sex contacts, analyze it, and validate it with data for chlamydia and gonorrhea; 2) to assess the percent increase in STI cases resulting from dating app use through a two-sex model for STIs and dating app use; 3) to appraise the positive impact of dating apps' pop-up ads may have in reducing STI incidence; and 4) to provide a tool to estimate the prevalence of STIs —thus filling in a large gap in available data that is usually difficult to measure directly.

2. Materials and methods

2.1. Important considerations

Data for STIs that must be reported to the Centers for Disease Control and Prevention (CDC) (chlamydia, gonorrhea, and syphilis) is quite detailed, mostly in the form of incidence but only occasionally as prevalence. Consequently, whenever we fit our models to data, it is for one or more of these three bacterial STIs.

We shall use throughout this article the following definitions of *disease prevalence* and *disease incidence* from the CDC [1].

Definition 1: number of cases of a disease (or infection) present at a given time is called *disease* (or *infection*) *prevalence* at that time.

Definition 2: rate of new cases of a disease (or infection) appearing at a given time (that is, the number of new cases per unit of time) is called *disease* (or *infection*) *incidence* at that time.

2.2. A simple two-sex SIS model

Generic epidemic models that assume homogeneity in the population are not directly applicable to sexually transmitted infections because the latter usually display large differences across sexes in some essential aspects of the transmission of infection, such as average number of sexual partners, transmissibility from one sex to another, use of protective barriers, etc. STIs may be transmitted by all types of sexual contact (oral, vaginal, and anal), through both same-sex and opposite-sex interactions.

Some of the oldest mathematical models for STIs correspond to gonorrhea, including an SI patch model without sex structure that contains nothing specific to STIs but is rather generally applicable to infectious diseases [11], and a lengthy set of 1984 lecture notes by Hethcote and Yorke that was published as a book and contains a section on heterosexual models of transmission [12].

A seminal paper in mathematical modeling of STIs because of its focus on pair formation dates back to 1988 [13]. In this article pairings are heterosexual and monogamous, and the model incorporates pair formation and dissolution/separation. The authors prove that, for that model, in order for an STI to be endemic, there needs to be a large enough separation rate to afford availability of enough new sexual partners. Since that time, some authors have been very prolific modeling different aspects of STI spread and focusing on some specific ones, for example M. Kretzschmar on chlamydia and gonorrhea. In [14], Kretzschmar introduced deterministic and stochastic models for the pair formation process in gonorrhea, setting a foundation for subsequent modeling endeavors. The research was further expanded in [15] through the use of stochastic network simulations to evaluate prevention strategies against gonorrhea and chlamydia. A comparative analysis of screening programs for chlamydia trachomatis was provided in [16], which expanded the scope of modeling to include chlamydia infections. The work continued in [17], where Kretzschmar delved into the impact of chlamydia screening initiatives, highlighting the predictive power of these models in the public health domain. This series culminates with [18], which contains refined models of pair formation for gonorrhea and also helps deepen our understanding of its transmission dynamics.

Many published models and studies are focused on the three main bacterial STIs: gonorrhea, chlamydia, and syphilis. For instance, [19] proposed three models aimed at enhancing syphilis screening and treatment within high-risk populations, and [20] presented a mathematical model of syphilis which provided deeper insights into the dynamics of the disease's transmission and the potential impact of intervention strategies. Additionally, since the advent of the HIV/AIDS epidemic, other models have specifically focused on STI transmission among men who have sex with men (MSM). For example, [21] introduced a new mathematical model of syphilis which shed light on its transmission dynamics and intervention strategies, [22] discussed behavioral interventions for HIV prevention among homosexual and bisexual men, and [23] developed an SIR epidemic model structured by immunological variables, enhancing understanding of disease progression and control. Transmission of STIs among women who have sex with women has been largely ignored, even though there is evidence that it is not negligible [24].

As far as we are able to ascertain, no mathematical models have been published incorporating both same-sex and opposite-sex transmission of STIs; that is what we do in this section. There are at least two different approaches to such mathematical models. One way is to divide the population of each sex into three mutually exclusive groups: individuals who have sexual relations exclusively with members of the other sex, those who have them exclusively with members of the same sex, and those who have them with both. Another, simpler approach than the first, involves summarizing the three types of sexual contact across sexes in averages for all individuals combined. We chose the latter approach because the former requires the model to have a much larger number of parameters and would pose very serious parameter identification problems given the scarcity of prevalence data for STIs. The main novelty of this modeling approach is that it allows us to obtain prevalence estimates without the need to structure the population by sexual preference into the six subgroups mentioned above.

We divide the sexually active population of size $N = N(t)$ into four compartments, according to the two essential conceptual axes related to sexually transmitted infections, namely sex and infection status. Accordingly, our model has the following four compartments: STI-susceptible females, STI-infected females, STI-susceptible males, and STI-infected males. Later, we shall subdivide these four compartments into two disjoint compartments each, one of dating app users, and another of non-users. The sizes of the four compartments will be denoted, respectively, as

$$S_f = S_f(t), \qquad I_f = I_f(t), \qquad S_m = S_m(t), \qquad I_m = I_m(t). \tag{2.1}$$

Because every individual is in exactly one of these compartments, it follows that

$$N = S_f + I_f + S_m + I_m. \tag{2.2}$$

We shall use the following notation $\big($with g representing sex, $g \in \{f, m\}\big)$:

$\xi_g =$ per capita exit rate from sexually active class of sex g for any reason,
$\gamma_g =$ per capita recovery rate for sex g by successful treatment or by spontaneous recovery,
$\Lambda_f =$ number of newly sexually active people who are female per unit time,
$\Lambda_m =$ number of newly sexually active people who are male per unit time,
$\lambda_g =$ per capita infection rate (*force of infection*) of sex-g susceptibles.

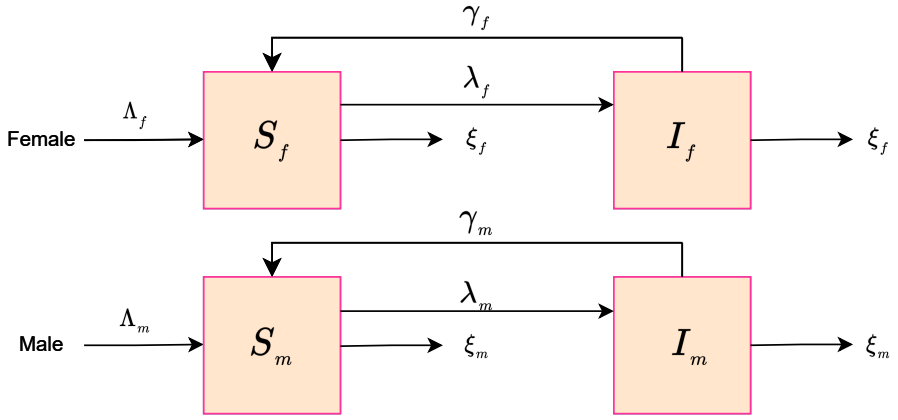

Figure 2. Flow diagram of the simple two-sex SIS model. Parameters over arrows are per capita rates, except for Λ_f and Λ_m, which are total rates.

We do not separate individuals of each sex into disjoint compartments according to their sexual-partner preferences, but we do want to consider same-sex and opposite-sex contacts. We use the following notation for transmission rates from each sex to the same and the opposite sexes: for $g_1, g_2 \in \{f, m\}$,

$$\begin{aligned} N_g &= \text{ total population size of sex } g, \\ \frac{C_{g_1 g_2}}{N_{g_2}} &= \text{ unit per capita infection transmission rate from sex } g_2 \text{ to sex } g_1. \end{aligned} \tag{2.3}$$

If we assume that average contact rates are not *density-dependent* (i.e., independent of group sizes) then we are led to the following constitutive form for the forces of infection, usually referred as *standard incidence*:

$$\lambda_f = C_{ff}\frac{I_f}{N_f} + C_{fm}\frac{I_m}{N_m}, \tag{2.4}$$

$$\lambda_m = C_{mm}\frac{I_m}{N_m} + C_{mf}\frac{I_f}{N_f}. \tag{2.5}$$

Figure 2 shows the flow diagram for our SIS model, where the parameters over each arrow are per capita transition rates, with the exception of the inflow parameters into susceptible compartments that represent total rates. Our SIS model describing the evolution of the four compartment sizes is given as

$$\begin{cases} \dfrac{d}{dt}S_f = \Lambda_f + \gamma_f I_f - \lambda_f S_f - \xi_f S_f, \\ \dfrac{d}{dt}I_f = \lambda_f S_f - \gamma_f I_f - \xi_f I_f, \\ \dfrac{d}{dt}S_m = \Lambda_m + \gamma_m I_m - \lambda_m S_m - \xi_m S_m, \\ \dfrac{d}{dt}I_m = \lambda_m S_m - \gamma_m I_m - \xi_m I_m, \end{cases} \tag{2.6}$$

where, summing the first two equations and the last two equations, we see that $F = N_f = S_f + I_f$ and $M = N_m = S_m + I_m$ satisfy the following "learning curve" ODEs

$$\frac{dF}{dt} = \Lambda_f - \xi_f F, \tag{2.7}$$

$$\frac{dM}{dt} = \Lambda_m - \xi_m M, \tag{2.8}$$

with solutions

$$F(t) = F(0)e^{-\xi_f t} + \frac{\Lambda_f}{\xi_f}(1 - e^{-\xi_f t}). \tag{2.9}$$

$$M(t) = M(0)e^{-\xi_m t} + \frac{\Lambda_m}{\xi_m}(1 - e^{-\xi_m t}), \tag{2.10}$$

2.2.1. Finding the initial conditions: S_f, S_m, I_f, and I_m

In order to run simulations using our model, ten parameters and four initial conditions need to be specified. We use the year 2009 as the initial one (corresponding to $t = 0$) so that we may compare model output with data for ten consecutive pre-pandemic years, 2010-2019. The years 2020 and 2021 were anomalous in terms of social and sexual contacts, and data for them should not be expected to fit well with output of autonomous dynamical systems such as those we use.

It is important to note that Definition 1 tells us the infection prevalence at a given time t is precisely the value of state variable $I(t)$, frequently reported as the proportion (percent) $I(t)/N(t)$. Similarly, Definition 2, when examined in view of (2.6), tells us that the infection incidence is precisely the value of $\lambda(t)S(t)$ = the acquisition rate of new infections at time t.

The initial conditions used for the number of susceptible and infected individuals of each sex are based on chlamydia prevalence data derived from the National Health and Nutrition Examination Survey (NHANES) [25]. The NHANES data is from 2007-2012, and was used as an approximation for 2009 data, which is not available. For each age group, STI prevalence was calculated by multiplying the prevalence percentage for that age group by the corresponding sexually active population data from 2009. Females and males were separated by multiplying the total population prevalence by the proportion of STI cases corresponding to females, X, and to males, $1 - X$, with STI incidence indicative of combined chlamydia, gonorrhea, and syphilis data. The proportions of prevalence for the sexes are

$$X = 0.733, \qquad 1 - X = 0.267. \tag{2.11}$$

Computations detailed above are displayed in Table 2. The values obtained for female and male prevalence were used as initial values for infected females and males in 2009, while the sizes of the susceptible compartments were estimated subtracting the initial numbers of infected for each sex from the total sexually active population of that sex.

In addition to the prevalence data collected from NHANES, the CDC provided information regarding the annual number of cases of chlamydia, gonorrhea, and syphilis for the years 2000-2021. Data

Table 2. Estimated female and male prevalence, 2009.

age	% prevalence	population (2009)	population prevalence	female prevalence	male prevalence
15-39	1.7	102,700,000	1,745,900	1,279,745	466,155
40+	0.4	137,000,000	548,000	401,684	146,316

was sub-grouped into total cases, female cases, and male cases. This data is indicative of STI incidence as there is no information given on the initial conditions for each STI. As such, the CDC data was discarded in favor of the prevalence statistics derived from the NHANES for the purpose of calculating the susceptible and infected compartments. This was done as prevalence data includes all STI cases that occur over a specified time period and, resultantly, is more strongly associated with STI transmission. Therefore, STI prevalence data is more pertinent for the aims of this study.

2.2.2. Estimation of epidemiological parameters: γ_g and $C_{g_1g_2}$

Of the ten model parameters, four can be obtained from demographic and other published data, namely:

Λ_f = number of newly sexually active people who are female per unit time
Λ_m = number of newly sexually active people who are male per unit time, and
ξ_f and ξ_m, whose reciprocals are the median durations of the sexual lives for sex $g = f, m$.

In [26], these were estimated to be

$$\Lambda_f = 3,777,794,\ \Lambda_m = 3,872,800,\ \xi_f = 0.0196,\ \xi_m = 0.0238. \tag{2.12}$$

Note that each of the *effective unit contact rates* $C_{g_1g_2}$ in (2.3) is a product of a behavioral parameter and an epidemiological one,

$$C_{g_1g_2} = \eta_{g_1g_2}\,\rho_{g_1g_2},$$

where

$\rho_{g_1g_2}$ = expected number (median) of sexual contacts per unit time of a person of sex g_2 with persons of sex g_1,

and

$\eta_{g_1g_2}$ = probability of an infected person of sex g_2 transmitting infection to a susceptible (uninfected) person of sex g_1 during a sexual contact (*transmissibility*).

The factors $\rho_{g_1g_2}$ and $\eta_{g_1g_2}$ making up each of the parameters $C_{g_1g_2}$ do not appear separately in our model, but rather only as their product; therefore, we do not need to identify them separately. The effective unit contact rates themselves will be identified by parameter fitting to incidence data.

However, the parameters $\rho_{g_1g_2}$ can be estimated using data for sexual identity-behavior [27]. Sexual identity in that study was given as 100% heterosexual, mostly straight/bisexual, or mostly gay/100% gay, while sexual behavior was defined as opposite sex only or both-sexes sex. The data for females aged 24-32 is given in Table 3 and for males aged 24-32 in Table 4. This data is compiled from answers to the questions "Considering all types of sexual activity, with how many male partners have you ever had sex?" and "Considering all types of sexual activity, with how many female partners have you ever had sex?"

Table 3. Females (24–32) Sexual Identity-Behavior.

		100% Heterosexual		Mostly Straight/Bisexual		Mostly Gay/100% Gay
	total sample	op. sex only	both sex sex	op. sex only	both sex sex	both sex sex
Respondents (N)	7392	5607	307	716	629	133
STI Rate	46.63	43.62	58.09	51.11	64.19	32
Sexual Partners (N)	10.41	7.7	15.84	11.63	27.7	16.5

Table 4. Males (24-32) Sexual Identity-Behavior.

		100% Heterosexual		Mostly Straight/Bisexual		Mostly Gay/100% Gay	
	total sample	op. sex only	both sex sex	op. sex only	both sex sex	same sex only	both sex sex
Respondents (N)	6323	5744	151	142	117	94	75
STI Rate	32.67	31.96	41.36	32.04	43.66	39.41	48.85
Sexual Partners (N)	17.64	17.1	20.21	12.09	26.92	37.45	29.47

The mean age for women in the study was 28.7, and 28.9 for men. The median age of sexual debut is estimated to be 17.2 for females and 16.8 for males [28]. We may estimate the average time since sexual debut for females in the study as $28.7 - 17.2 = 11.5$, and for males as $28.9 - 16.8 = 12.1$.

We compute now the median numbers of sexual partners of each sex that sexually active women had had, of the opposite sex, a_f —as the weighted average of the numbers of partners reported in columns 3 and 5 of Table 3— and of the same sex, b_f —as the weighted average of the numbers of partners reported in columns 4, 6, and 7 of Table 3:

$$a_f = \left(\frac{5607}{5607+716}\right)\cdot(7.7) + \left(\frac{716}{5607+716}\right)\cdot(11.63) \approx 8.15.$$

$$b_f = \left(\frac{307}{307+629+133}\right)\cdot(15.84) + \left(\frac{629}{307+629+133}\right)\cdot(27.7) + \left(\frac{133}{307+629+133}\right)\cdot(16.5) \approx 22.9.$$

Finally, we compute the annual numbers as the ratios of these to the median time-span of their sexually active life:

$$\rho_{fm} = \frac{8.15}{11.5} \approx 0.709, \qquad \rho_{ff} = \frac{22.9}{11.5} \approx 1.99. \tag{2.13}$$

Similarly, we compute the median numbers of sexual partners that sexually active men had had, of the opposite sex, a_m —as the weighted average of the numbers of partners reported in columns 3 and 5

of Table 4— and of the same sex, b_m —as the weighted average of the numbers of partners reported in columns 4, 6, 7, and 8 of Table 4:

$$a_m = \left(\frac{5744}{5744+142}\right)\cdot(17.1) + \left(\frac{142}{5744+142}\right)\cdot(12.09) \approx 17.0$$

$$b_m = \frac{1}{437}[(151)\cdot(20.21) + (117)\cdot(26.92) + (94)\cdot(37.45) + (75)\cdot(29.47)] \approx 27.3.$$

Now, we may compute the annual numbers for men as ratios of these to the median time-span of their sexually active life:

$$\rho_{mf} = \frac{17.0}{12.1} \approx 1.40, \qquad \rho_{mm} = \frac{27.3}{12.1} \approx 2.26. \tag{2.14}$$

The *sexual preference* parameters, ν_g, are the fractions of all sexual contacts of persons of sex g that are with persons of the opposite sex (they can separate same-sex contacts from opposite-sex contacts):

$$\nu_f = \frac{a_f\cdot 6323}{a_f\cdot 6323 + b_f\cdot 1069} \approx 67.8\%, \qquad \nu_m = \frac{a_m\cdot 5886}{a_m\cdot 5886 + b_m\cdot 437} \approx 89.3\%. \tag{2.15}$$

Concerning the parameters $\eta_{g_1g_2}$, there is some scattered information for the three STIs of our study, for example, [29] reports chlamydial $\eta_{g_1g_2} = 0.022 - 0.044$ for the four types of sexual partnerships combined. On the other hand, [30] reports some probabilities of transmission per type of sex act for gonorrhea that can be combined as: $\eta_{fm} = 0.5 - 0.84$, $\eta_{mf} = 0.02 - 0.2$, and $\eta_{mm} = 0.63 - 0.84$. We see that wide ranges of values and disparate orders of magnitude for different STIs have been reported. Therefore, we decided to identify the transmissibilities for our model (together with the per capita recovery rates) by fitting them to incidence data. Still, for reference purposes, we compute them from the values of ρ and η given above:

$$C_{ff} \approx 1.99(0.033) = 0.00657, \qquad C_{fm} \approx 0.709(0.6) = 0.0395, \tag{2.16}$$

$$C_{mf} \approx 1.40(0.05) = 0.07, \qquad C_{mm} \approx 2.26(0.7) = 1.58. \tag{2.17}$$

In the end, the parameters representing unit effective contact rates and per capita recovery rates of our model (2.6) were fitted to available annual data of incidence of gonorrhea by sex. We fitted those 6 parameters to five years of incidence data (2014-2019, with 10 data points in total). The fitting of the model to incidence data was performed using the routine "lsqcurvefit" in the software MATLAB, which determined the parameter values $(\gamma_f, \gamma_m, C_{ff}, C_{fm}, C_{mm}, C_{mf})$ that minimize the sum of the relative squared deviations between incidence data for each year for each sex and the corresponding model-estimated incidence. The results of the parameter fitting are shown in Figures 6 and 7, and the estimated parameter values, together with the initial conditions and the four fixed parameter values obtained in (2.12), are presented in Table 5.

2.2.3. Other important epidemiological parameters

Note that the parameters ξ_g can be expressed as sums of the per capita mortality rates for each sex, μ_g, and an additional exit rate from the sexually active population for reasons other than death, κ_g,

$$\xi_g = \mu_g + \kappa_g.$$

The reciprocals of the parameters μ_g represent the median (expected value) of the remaining life of people of sex g in the sexually active population (i.e. *life expectancy* at age 15). These can be obtained from life tables [31], $1/\mu_f = 66.8$ and $1/\mu_g = 62.1$. Thus,

$$\mu_f = 0.0150, \qquad \mu_m = 0.0161. \tag{2.18}$$

The reciprocals of the parameters ξ_g represent the median (expected value) of the permanence of people of sex g in the sexually active population (*length of sexual life*). They have been estimated from sexually active population data (see (2.12)), giving us $1/0.0196 \approx 51.0$ years for women and $1/0.0238 \approx 42.0$ for men. From them, we may obtain estimates for $\kappa_g = \xi_g - \mu_g$ (that are not really needed):

$$\kappa_f = 0.0196 - 0.0150 \approx 0.0046, \qquad \kappa_m = 0.0238 - 0.0161 \approx 0.0077. \tag{2.19}$$

The reciprocals of the parameters γ_g represent the median (expected value) of the duration of infection for infected people of sex g. The duration of infection may differ significantly among those infected because of the different courses that infection may follow for different individuals. Infected people may be symptomatic or asymptomatic. The former may or may not seek treatment, while the latter may or may not recover spontaneously. The asymptomatic who do not recover spontaneously may discover their infection through screening.

2.3. An STI SIS model for dating app users

We now assign the individuals of each sex to compartments based on the two factors that are at the center of this study, namely dating application status (user vs. non-user) and infection status (susceptible vs. infected) for the two most common, curable, bacterial STIs (chlamydia and gonorrhea). Thus our model has the following eight compartments: susceptible female users of dating apps, infected female users of dating apps, susceptible male users of dating apps, infected male users of dating apps, susceptible female non-users of dating apps, infected female non-users of dating apps, susceptible male non-users of dating apps, infected male non-users of dating apps. The sizes of these compartments will be denoted, respectively, as

$$S_f^u = S_f^u(t), \qquad I_f^u = I_f^u(t), \qquad S_m^u = S_m^u(t), \qquad I_m^u = I_m^u(t), \tag{2.20}$$

$$S_f^{nu} = S_f^{nu}(t), \quad I_f^{nu} = I_f^{nu}(t), \quad S_m^{nu} = S_m^{nu}(t), \quad I_m^{nu} = I_m^{nu}(t), \tag{2.21}$$

with the total populations by sex and dating app status denoted by

$$N_f^n = S_f^n + I_f^n, \qquad N_f^u = S_f^u + I_f^u, \qquad N_m^n = S_m^n + I_m^n, \qquad N_m^u = S_m^u + I_f^u m. \tag{2.22}$$

Because every individual is in exactly one of these compartments, it follows that

$$N = S_f^u + I_f^u + S_m^u + I_m^u + S_f^{nu} + I_f^{nu} + S_m^{nu} + I_m^{nu}. \tag{2.23}$$

We shall keep the meaning of the parameters Λ_g and ξ_g (because they are demographic, independent of app use and infection) and introduce the notation, for $s = n, u$,

$\Lambda_g^s =$ number of newly sexually active people entering compartment of sex g and app user status s,
$\gamma_g^s =$ per capita recovery rate in compartment of sex g and app user status s,
$\lambda_g^s =$ per capita infection rate (*force of infection*) in compartment of sex g and app user status s.

In this setting, unlike in our simple SIS model (2.6), we formally model opposite-sex contacts only. Same-sex contacts are not considered separately due to a lack of data of sexual partners by dating app usage, and also to avoid the need for an additional 8 constants (the effective same-sex contact rates by infection and dating-app-use status. This may not affect our conclusions too much because, for individuals of each sex, the proportion of same-sex contacts is fairly small within all their sexual contacts.

Consequently, the constitutive form of the forces of infection are given by

$$\begin{aligned}
\lambda_f^n &= C_{fm}^{nn}\frac{I_m^n}{N_m^n} + C_{fm}^{nu}\frac{I_m^u}{N_m^u},\\
\lambda_m^n &= C_{mf}^{nn}\frac{I_f^n}{N_f^n} + C_{mf}^{nu}\frac{I_f^u}{N_f^u},\\
\lambda_f^u &= C_{fm}^{un}\frac{I_m^n}{N_m^n} + C_{fm}^{uu}\frac{I_m^u}{N_m^u},\\
\lambda_m^u &= C_{mf}^{un}\frac{I_f^n}{N_f^n} + C_{mf}^{uu}\frac{I_f^u}{N_f^u},
\end{aligned} \tag{2.24}$$

where, for $g_1, g_2 \in \{f, m\}$, $s_1, s_2 \in \{u, n\}$,

$$0 < C_{g_1g_2}^{s_1s_2} = \text{ unit per capita infectivity from sex } g_2 \text{ and status } s_2 \text{ to sex } g_1 \text{ and status } s_1. \tag{2.25}$$

Furthermore, we shall assume that the initial, non-negative compartment sizes satisfy the following condition:

$$\sum_{g,s} I_g^s(0) > 0 \tag{2.26}$$

so that there is STI transmission.

Figure 3 shows the flow diagram for our dating app model, where the parameters over each arrow are per capita transition rates, with the exception of the inflow parameters into susceptible compartments that represent total rates. Our dynamical system model describing the evolution of the compartment sizes is as follows:

$$\frac{d}{dt}S_f^n = \Lambda_f^n + \gamma_f^n I_f^n - \lambda_f^n S_f^n - \xi_f S_f^n, \tag{2.27}$$

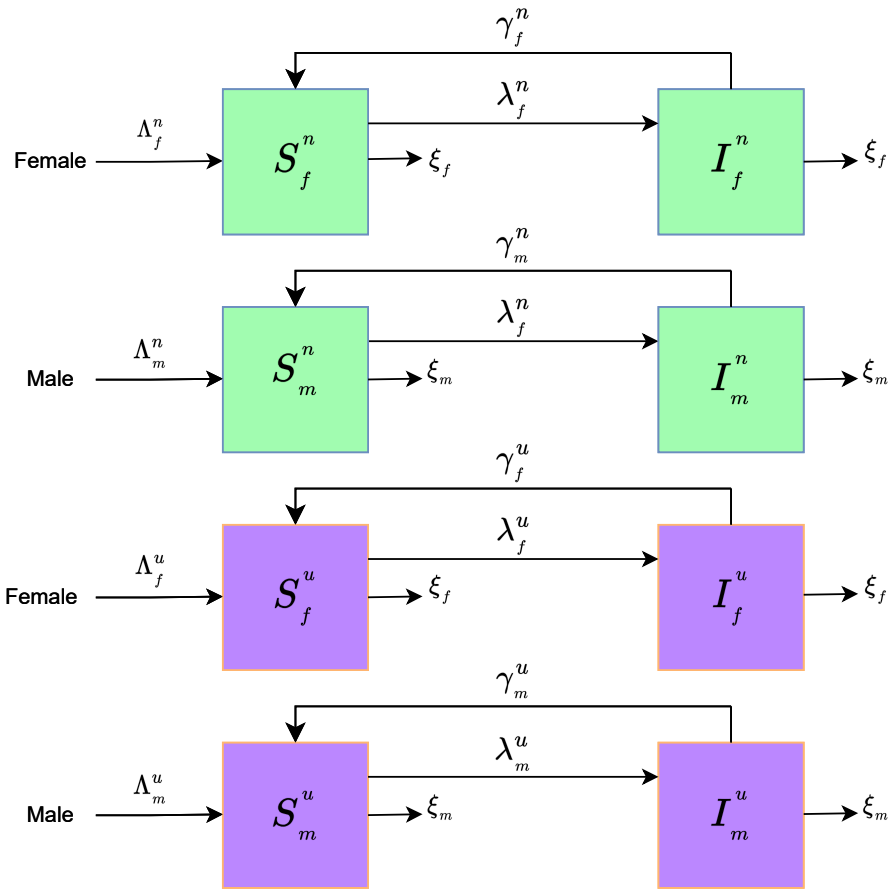

Figure 3. Flow diagram of our dating app STI model. The parameters over the arrows are per capita rates, except for inflow parameters into susceptible compartments that represent total rates.

$$\frac{d}{dt}I_f^n = \lambda_f^n S_f^n - \xi_f I_f^n - \gamma_f^n I_f^n, \tag{2.28}$$

$$\frac{d}{dt}S_m^n = \Lambda_m^n + \gamma_m^n I_m^n - \lambda_m^n S_m^n - \xi_m S_m^n, \tag{2.29}$$

$$\frac{d}{dt}I_m^n = \lambda_m^n S_m^n - \xi_m I_m^n - \gamma_m^n I_m^n, \tag{2.30}$$

$$\frac{d}{dt}S_f^u = \Lambda_f^u + \gamma_f^u I_f^u - \lambda_f^u S_f^u - \xi_f S_f^u, \tag{2.31}$$

$$\frac{d}{dt}I_f^u = \lambda_f^u S_f^u - \xi_f I_f^u - \gamma_f^u I_f^u, \tag{2.32}$$

$$\frac{d}{dt}S_m^u = \Lambda_m^u + \gamma_m^u I_m^u - \lambda_m^u S_m^u - \xi_m S_m^u, \tag{2.33}$$

$$\frac{d}{dt}I_m^u = \lambda_m^u S_m^u - \xi_m I_m^u - \gamma_m^u I_m^u. \tag{2.34}$$

2.3.1. Parameter estimation

Note that our 8-compartment STI SIS model for dating app users, (2.27)–(2.34), involves 6 demographic parameters and 8 initial conditions that were identified or are easily derived from the simple two-sex SIS model, namely $\Lambda_f^n, \Lambda_m^n, \Lambda_f^u, \Lambda_m^u, \xi_f$, and ξ_m, and $S_f^n(0)$, $S_f^u(0)$, $S_m^n(0)$, $S_m^u(0)$, $I_f^n(0)$, $I_f^u(0)$, $I_m^n(0)$, and $I_m^u(0)$. For that model we actually identified $\Lambda_f = \Lambda_f^n + \Lambda_f^u$ and $\Lambda_m = \Lambda_m^n + \Lambda_m^u$, which we now separated into app-user and non-user based on the percentages of each of these statuses derived from data contained in [5]. The 8 initial conditions were chosen as those from the simple SIS model (see section 2.2.1), $S_f(0)$, $S_m(0)$, $I_f(0)$, and $I_m(0)$, separated now into app-user and non-user based on the percentages of each of these statuses derived from data contained in [5].

The 12 epidemiological parameters were fitted to (STI —chlamydia/gonorrhea) incidence data by sex using MATLAB, specifically the routine "fminsearch" to minimize the maximum of the relative deviations between incidence data and the corresponding model output values.

2.3.2. Sensitivity analyses and other simulations

Local and global sensitivity analyses were conducted utilizing MATLAB and its integrated packages. The local sensitivity analysis involved increasing the value of a single parameter by 1%, with all other parameters remaining constant at their values derived from data, followed by the computation of the percentage change in both incidence and prevalence relative to the baseline values. This process was repeated for various values of the selected parameter to construct sensitivity curves. The data-derived parameter value was then highlighted as a red point on these curves (refer to Figures 12 and 13, for examples). Conversely, global sensitivity analyses were performed via Partial Rank Correlation Analysis (PRCA). This entailed sampling one million sets of parameter values utilizing Latin Hypercube Sampling (LHS), which were subsequently employed to simulate the model over a decade. The sets of parameters, alongside the incidence and prevalence derived from the simulations, served as inputs to the MATLAB function "partialcorr". This step facilitated the acquisition of correlation coefficients for each parameter, assessing their impact on the incidence and prevalence of sexually transmitted infections (see Figure 16 for an example). The same approach was utilized to assess the impact of dating app users on the incidence and prevalence of STIs.

Scenario analyses were conducted to evaluate the potential effects of integrating advertising campaigns into dating apps aimed at mitigating risky sexual behaviors, such as decreased condom use or an increase in the number of sexual partners. These scenarios were based on diminishing either the average duration of stay in the infectious class, denoted as $\frac{1}{\gamma}$, or the per capita rate of STI transmission from sex g_2 and status s_2 to sex g_1 and status s_1, represented by $C_{g_1g_2}^{s_1s_2}$. The parameters $C_{g_1g_2}^{uu}$ were reduced by 10% to 40%, starting in 2019, to examine their influence on the prevalence and incidence among males and females from 2019 to 2021. This assessment was carried out for each possible pairing of sexes g_1, g_2 (refer to Figure 18 for an example).

3. Results and discussion

3.1. Simple SIS model results

We present several analytical findings in conjunction with the outcomes of parameter estimation for this simplified model, achieved by fitting the model to five years of incidence data.

3.1.1. Invariance of a positive cone

We prove that solutions that begin non-negative, stay non-negative and are bounded for all time.

We know that the functions F = number of sexually active females and M = number of sexually active males, have graphs shaped like learning curves, i.e. concave (convex if $F(0) > \Lambda_f/\xi_f$, respectively $M(0) > \Lambda_m/\xi_m$) functions that increase (decrease if convex) monotonically from their initial values $F(0)$ and $M(0)$ to their asymptotic values $F_\infty = \Lambda_f/\xi_f$ and $M_\infty = \Lambda_m/\xi_m$, respectively.

Moreover, (2.9) and (2.10) imply that F is bounded by $\max\left\{F(0), \frac{\Lambda_f}{\xi_f}\right\}$ and M is bounded by $\max\left\{M(0), \frac{\Lambda_m}{\xi_m}\right\}$. Similarly, we have a learning curve model for the total population N by letting

$$\Lambda = \Lambda_f + \Lambda_m, \qquad \xi = \frac{\Lambda_f + \Lambda_m}{\frac{\Lambda_f}{\xi_f} + \frac{\Lambda_m}{\xi_m}},$$

where its asymptotic value is given by

$$N_\infty = F_\infty + M_\infty = \frac{\Lambda_f}{\xi_f} + \frac{\Lambda_m}{\xi_m} = \frac{\Lambda}{\xi}. \tag{3.1}$$

Thus we see that N is defined for all $t \geq 0$, is bounded above, and bounded away from 0. Therefore, the existence and uniqueness theorem for systems of ODEs guarantees the existence of a global unique solution to system (2.6) for any initial conditions.

Theorem 3.1. *The cone* $\left\{(S_f, I_f, S_m, I_m) \in \mathbb{R}^4 : S_f, I_f, S_m, I_m \geq 0,\ S_f + I_f + S_m + I_m \leq \frac{\Lambda_f}{\xi_f} + \frac{\Lambda_m}{\xi_m}\right\}$ *is invariant and attractive under the flow of system* (2.6).

Proof: We first discard the trivial cases that have no infected individuals initially (i.e. $I_f(0) = I_m(0) = 0$). In that case, by uniqueness of solutions, the susceptible class of each sex evolves demographically according to the learning curve equations (2.9) and (2.10), while the infected classes are empty at all times (i.e., $I_f \equiv 0$ and $I_m \equiv 0$).

We then assume that at least one the infected classes is initially non-empty. Without loss of generality let,

$$I_f(0) > 0. \tag{3.2}$$

It follows from (2.4) that $\lambda_f(0), \lambda_m(0) > 0$, and, by continuity, there is $\tilde{t} > 0$ such that

$$\lambda_f(t), \lambda_m(t) > 0, \qquad \text{for all } t \in [0.\tilde{t}). \tag{3.3}$$

Note that the equations for susceptibles in (2.6) imply that, for $t \in (0, \tilde{t})$ and $g = f, m$,

$$\frac{d}{dt}\left(S_g\, e^{\xi_g t + \int_0^t \lambda_g(\tau)d\tau}\right) = \left[\Lambda_g + \gamma_g I_g(t)\right] e^{\xi_g t + \int_0^t \lambda_g(\tau)d\tau} > 0, \tag{3.4}$$

whereby

$$S_g(t)\, e^{\xi_g t + \int_0^t \lambda_g(\tau)d\tau} - S_g(0) = \Lambda_g \int_0^t e^{\xi_g v + \int_0^v \lambda_g(\tau)d\tau} dv + \gamma_g \int_0^t I_g(v)\, e^{\xi_g v + \int_0^v \lambda_g(\tau)d\tau} dv > 0.$$

Hence, for all $t \in (0, \tilde{t})$ and $g = f, m$,

$$S_g(t) = S_g(0)\, e^{-\xi_g t - \int_0^t \lambda_g(\tau)d\tau} + \int_0^t \left[\Lambda_g + \gamma_g I_g(v)\right] e^{-\xi_g (t-v) - \int_v^t \lambda_g(\tau)d\tau} dv > 0. \tag{3.5}$$

Similarly, starting from the equations for infected persons in (2.6) and writing the analogue of (3.4) for them, we can see that for all $t \in (0, \tilde{t})$ and $g = f, m$,

$$I_g(t) = I_g(0)\, e^{-(\xi_g + \gamma_g)t} + \int_0^t e^{-(\xi_g + \gamma_g)(t-\tau)} \lambda_g(\tau) S_g(\tau) d\tau > 0. \tag{3.6}$$

Then, collecting (3.3), (3.5), and (3.6), for $t \in (0, \tilde{t})$ we have

$$S_f(t), I_f(t), S_m(t), I_m(t), \lambda_f, \lambda_m > 0. \tag{3.7}$$

We need to prove that the four compartments of N stay non-negative for all time. Suppose they do not, and let t^* be the first positive time at which one of the four becomes empty ($t^* \geq \tilde{t}$ by (3.7)):

$$t^* = \inf\{t > 0 : S_f(t) \cdot S_m(t) \cdot I_f(t) \cdot I_m(t) = 0\}. \tag{3.8}$$

Note that (3.8) implies that

$$S_f(t), I_f(t), S_m(t), I_m(t), \lambda_f(t), \lambda_m(t) > 0 \ \text{ for all } \ t \in (0, t^*). \tag{3.9}$$

Combining (3.5), (3.6), and (3.9), we see that

$$S_f(t^*), I_f(t^*), S_m(t^*), I_m(t^*), \lambda_f(t^*), \lambda_m(t^*) > 0$$

This contradicts the assumption (3.8) on t^*, establishing that the solutions cannot vanish at any positive time. The upper bound now follows from (2.2) and (3.1), thus concluding the proof. □

3.1.2. Steady states and their stability

We will now focus on equilibrium solutions of the system and their stability. We see from (2.6) that any equilibrium $E^* = (S_f^*, I_f^*, S_m^*, I_m^*)$ must satisfy

$$S_f^* + I_f^* = F_\infty = \frac{\Lambda_f}{\xi_f}, \qquad S_m^* + I_m^* = M_\infty = \frac{\Lambda_m}{\xi_m}. \tag{3.10}$$

For the systems representing each of the sexes *in the absence of the other* -the first two equations of (2.6) for females, and the last two equations of (2.6) for males- we have the basic reproduction numbers

$$\mathcal{R}_0^f = \frac{C_{ff}}{\xi_f + \gamma_f} \qquad \text{and} \qquad \mathcal{R}_0^m = \frac{C_{mm}}{\xi_m + \gamma_m}. \tag{3.11}$$

The basic reproduction number of an epidemic generalizes the more general concept of basic reproduction number of a population [32], and it is "the number of secondary cases produced, in a totally susceptible population, by a single infective individual during the time span of the infection". [32]

When we consider only transmission within the same sex, the resulting single-sex systems of females and males each have a disease-free equilibrium

$$(S_g^*,\, I_g^*) = \left(\frac{\Lambda_g}{\xi_g}, 0\right), \qquad g = f, m, \tag{3.12}$$

and a unique endemic one that lies in the positive quadrant if, and only if, $\mathcal{R}_0^g = \dfrac{C_{gg}}{\gamma_g + \xi_g} > 1$,

$$(\bar{S}_g, \bar{I}_g) = \left(\frac{(\xi_g + \gamma_g)\Lambda_g}{C_{gg}\xi_g}, \frac{\Lambda_g}{\xi_g}\left(1 - \frac{\xi_g + \gamma_g}{C_{gg}}\right)\right) = \left(\frac{\Lambda_g}{\xi_- g}\,\frac{1}{\mathcal{R}_0^g}\,,\, \frac{\Lambda_g}{\xi_g}\left(1 - \frac{1}{\mathcal{R}_0^g}\right)\right).$$

We have the following known stability results.

Theorem 3.2. *[33] The disease-free equilibrium* (S_g^*, I_g^*) *of the single-sex model is globally asymptotically stable if* $\mathcal{R}_0^g \le 1$ *and unstable if* $\mathcal{R}_0^g > 1$. *In the latter case, the endemic equilibrium* $(\bar{S}_g, \bar{I}_g)$ *is globally asymptotically stable.*

Concerning the coupled two-sex SIS system, the relation (3.10) together with (2.6) readily lead to trivial ('infection-free') and two boundary ('only-one-sex-infected') equilibria. Setting $\xi = \frac{\xi_f \xi_m \Lambda}{\Lambda_f \xi_m + \Lambda_m \xi_f}$ and the total population $\bar{N} = F_\infty + M_\infty = \frac{\Lambda_f}{\xi_f} + \frac{\Lambda_m}{\xi_m} = \frac{\Lambda}{\xi}$,

$$E_0 = \left(\frac{\Lambda_f}{\xi_f},\ 0,\ \frac{\Lambda_m}{\xi_m},\ 0\right) = (F_\infty,\ 0,\ M_\infty,\ 0)\,, \tag{3.13}$$

$$E_f^* = \left(\frac{F_\infty}{\mathcal{R}_0^f}, F_\infty\left(1 - \frac{1}{\mathcal{R}_0^f}\right), M_\infty, 0\right), \qquad E_m^* = \left(F_\infty, 0, \frac{M_\infty}{\mathcal{R}_0^m}, M_\infty\left(1 - \frac{1}{\mathcal{R}_0^m}\right)\right), \tag{3.14}$$

the latter two being meaningful (i.e. non-negative and different from E_0) if, and only if, respectively,

$$\mathcal{R}_0^f > 1, \qquad \text{or} \qquad \mathcal{R}_0^m > 1. \tag{3.15}$$

When only one sex is present (i.e. either $F_\infty = 0$ or $M_\infty = 0$), (3.15) is exactly (3.11).

We will prove next a classical threshold condition for the stability of the disease-free equilibrium, see for example [34]. We begin by computing the basic reproduction number $\mathcal{R}_0$ = spectral radius of

the next generation matrix [34],

$$G = \begin{pmatrix} \mathcal{R}_0^f & \dfrac{C_{fm}}{C_{mm}}\dfrac{F_\infty}{M_\infty}\mathcal{R}_0^m \\ \dfrac{C_{mf}}{C_{ff}}\dfrac{M_\infty}{F_\infty}\mathcal{R}_0^f & \mathcal{R}_0^m \end{pmatrix} = \begin{pmatrix} a & b \\ c & d \end{pmatrix}.$$

Because the off-diagonal coefficients of G have the same sign (they are both non-negative), G has two real non-negative eigenvalues,

$$0 \leq \frac{a+d}{2} - \frac{\sqrt{(a+d)^2 - 4(ad-bc)}}{2} \leq \frac{a+d}{2} + \frac{\sqrt{(a+d)^2 - 4(ad-bc)}}{2}.$$

Indeed, this follows because the discriminant $(\mathrm{tr}(G))^2 - 4\det(G) = (a-d)^2 + 4bc \geq 0$. Therefore,

$$\mathcal{R}_0 = \frac{\mathrm{tr}(G)}{2} + \sqrt{\frac{\mathrm{tr}^2(G)}{4} - \det(G)} = \frac{1}{2}\left(\mathcal{R}_0^f + \mathcal{R}_0^m + \sqrt{\left(\mathcal{R}_0^f - \mathcal{R}_0^m\right)^2 + 4\mathcal{R}_0^f\mathcal{R}_0^m\,\frac{C_{fm}C_{mf}}{C_{ff}C_{mm}}}\right). \tag{3.16}$$

In general, the next generation matrix is computed as the product of the *transmission matrix* containing the unit transmission rates across infectious classes, and the inverse of the *transition matrix* containing the unit transition rates to non-infectious classes. This matrix product generalizes the simplest expression for $\mathcal{R}_0$ in the case of an unstructured population as the product of the unit transmission rate and the reciprocal of the unit recovery rate that represents the mean infectious period. The next generation matrix being positive, its spectral radius is its largest eigenvalue.

Theorem 3.3. *(see [34]) The equilibrium E_0 is locally asymptotically stable if $\mathcal{R}_0 < 1$ and unstable if $\mathcal{R}_0 > 1$.*

Proof: First, note that the threshold condition $\mathcal{R}_0 < 1$ is equivalent to

$$\mathrm{tr}^2(G) - 4\det(G) < (2 - \mathrm{tr}(G))^2,$$

that is,

$$\boxed{\mathcal{R}_0 < 1 \iff 1 - \mathrm{tr}(G) + \det(G) > 0}. \tag{3.17}$$

The Jacobian matrix of system (2.6) is

$$J(S_f, I_f, S_m, I_m) = \begin{pmatrix} -\xi_f - \lambda_f & \gamma_f - \dfrac{C_{ff}}{F_\infty}S_f & 0 & -\dfrac{C_{fm}}{M_\infty}S_f \\ \lambda_f & \dfrac{C_{ff}}{F_\infty}S_f - \xi_f - \gamma_f & 0 & \dfrac{C_{fm}}{M_\infty}S_f \\ 0 & -\dfrac{C_{mf}}{F_\infty}S_m & -\xi_m - \lambda_m & \gamma_m - \dfrac{C_{mm}}{M_\infty}S_m \\ 0 & \dfrac{C_{mf}}{F_\infty}S_m & \lambda_m & \dfrac{C_{mm}}{M_\infty}S_m - \xi_m - \gamma_m \end{pmatrix}. \tag{3.18}$$

Evaluating (3.18) at E_0,

$$J(E_0) = \begin{pmatrix} -\xi_f & \gamma_f - C_{ff} & 0 & -C_{fm}\dfrac{F_\infty}{M_\infty} \\ 0 & C_{ff} - \xi_f - \gamma_f & 0 & C_{fm}\dfrac{F_\infty}{M_\infty} \\ 0 & -C_{mf}\dfrac{M_\infty}{F_\infty} & -\xi_m & \gamma_m - C_{mm} \\ 0 & C_{mf}\dfrac{M_\infty}{F_\infty} & 0 & C_{mm} - \xi_m - \gamma_m \end{pmatrix}.$$

The eigenvalues of $J(E_0)$ are the two negative real numbers,

$$-\xi_f, \quad -\xi_m,$$

and the two eigenvalues of the matrix

$$A = \begin{pmatrix} C_{ff} - \xi_f - \gamma_f & C_{fm}\dfrac{F_\infty}{M_\infty} \\ C_{mf}\dfrac{M_\infty}{F_\infty} & C_{mm} - \xi_m - \gamma_m \end{pmatrix} = \begin{pmatrix} (\xi_f + \gamma_f)(\mathcal{R}_0^f - 1) & \dfrac{C_{fm}}{C_{ff}}(\xi_f + \gamma_f)\mathcal{R}_0^f \\ \dfrac{C_{mf}}{C_{mm}}(\xi_m + \gamma_m)\mathcal{R}_0^m & (\xi_m + \gamma_m)(\mathcal{R}_0^m - 1) \end{pmatrix},$$

which have negative real part if, and only if,

$$\mathrm{tr}(A) < 0 \quad \text{and} \quad \det(A) > 0. \tag{3.19}$$

The second condition in (3.19) is equivalent to

$$(a-1)(d-1) - bc = \det(G) - \mathrm{tr}(G) + 1 > 0,$$

which, by (3.17), is equivalent to $\mathcal{R}_0 < 1$. Then, *a fortiori* $(a-1)(d-1) > bc \geq 0$, and $a-1$ and $d-1$ have the same sign. Also note that, in view of (3.16), the condition $\mathcal{R}_0 < 1$ implies that

$$\frac{a+d}{2} < 1,$$

whereby $(a-1) + (d-1) < 0$, and then $a - 1 < 0$ or $d - 1 < 0$. Because they have the same sign, it follows that

$$a - 1 < 0 \ \text{ and } \ d - 1 < 0. \tag{3.20}$$

The first condition in (3.19) is

$$(a-1)(\xi_f + \gamma_f) + (d-1)(\xi_m + \gamma_m) < 0,$$

which follows immediately from (3.20).

This proves the stability part of the theorem. The instability follows immediately from

$$\boxed{\mathcal{R}_0 > 1 \iff 1 - \mathrm{tr}(G) + \det(G) < 0 \iff \det(A) < 0}\,. \tag{3.21}$$

□

We note that (3.20) can be restated as

$$\mathcal{R}_0 < 1 \Longrightarrow \mathcal{R}_0^f < 1 \text{ and } \mathcal{R}_0^m < 1. \tag{3.22}$$

Now we turn our attention to the 'only-one-sex-infected' equilibria. We prove here the classical threshold stability result for E_f^* and omit it for E_m^*, because its proof is essentially identical to the one for E_f^*.

Theorem 3.4. *The equilibrium E_f^* is locally asymptotically stable if $\mathcal{R}_0^f > 1$ and $\mathcal{R}_0^m < 1$. It is unstable if $\mathcal{R}_0^f < 1$ or $\mathcal{R}_0^m > 1$.*

Proof: First, recall that for E_f^* to be distinct from E_0, we need to assume $C_{mf} = 0$, i.e. $\lambda_m = 0$. Therefore, the Jacobian matrix at E_f^*, (3.18), is

$$J\left(\frac{F_\infty}{\mathcal{R}_0^f}, F_\infty\left(1 - \frac{1}{\mathcal{R}_0^f}\right), M_\infty, 0\right) = \begin{pmatrix} -\xi_f - \lambda_f & -\xi_f & 0 & -\dfrac{C_{fm}}{\mathcal{R}_0^f}\dfrac{F_\infty}{M_\infty} \\ (\gamma_f + \xi_f)\,(\mathcal{R}_0^f - 1) & 0 & 0 & \dfrac{C_{fm}}{\mathcal{R}_0^f}\dfrac{F_\infty}{M_\infty} \\ 0 & 0 & -\xi_m & \gamma_m - C_{mm} \\ 0 & 0 & 0 & (\gamma_m + \xi_m)(\mathcal{R}_0^m - 1) \end{pmatrix}. \tag{3.23}$$

The structure of (3.23) tells us that the eigenvalues of this Jacobian for $\mathcal{R}_0^f > 1$ and $\mathcal{R}_0^m < 1$ are

$$-\xi_m, \quad (\gamma_m + \xi_m)(\mathcal{R}_0^m - 1),$$

both of which are real and negative, and the two eigenvalues of

$$M_1 = \begin{pmatrix} -\xi_f - \lambda_f & -\xi_f \\ (\gamma_f + \xi_f)\,(\mathcal{R}_0^f - 1) & 0 \end{pmatrix}, \tag{3.24}$$

both have a negative real part because $\mathrm{tr}(M_1) < 0$ and $\det(M_1) > 0$. The instability result follows by noting that $\mathcal{R}_0^m > 1$ is equivalent to $(\gamma_m + \xi_m)(\mathcal{R}_0^m - 1) > 0$, while $\mathcal{R}_0^f < 1$ is equivalent to $\det(M_1) < 0$ [34]. □

Note that Theorem 3.4 together with (3.22) say that a necessary condition for the stability of E_f^* is $\mathcal{R}_0 > 1$. However, this condition is not sufficient.

As we indicated earlier, because of (3.10), all steady states of system (2.6) are determined by solving for the infected-equilibrium conditions

$$\left(\frac{C_{ff}I_f^*}{F_\infty}+\frac{C_{fm}I_m^*}{M_\infty}\right)(F_\infty-I_f^*)-\gamma_f I_f^*-\xi_f I_f^*=\left(\frac{C_{mf}I_f^*}{F_\infty}+\frac{C_{mm}I_m^*}{M_\infty}\right)(M_\infty-I_m^*)-\gamma_m I_m^*-\xi_m I_m^*=0. \quad (3.25)$$

We see from (3.25) that

$$I_m^*=0 \iff I_f^*=0 \text{ or } C_{mf}=0,$$

which correspond, respectively, to the disease-free equilibrium E_0 and to the 'only-females-infected' equilibrium E_f^* in (3.14), while

$$I_f^*=0 \iff I_m^*=0 \text{ or } C_{fm}=0,$$

which correspond, respectively, to the disease-free equilibrium E_0 and to the 'only-males-infected' equilibrium E_m^* in (3.14).

We are now ready to find the positive equilibria, with both sexes infected. Solving the first equation of (3.25) for I_m^*,

$$I_m^*=\frac{((\gamma_f+\xi_f)-\frac{C_{ff}}{F_\infty}(F_\infty-I_f^*))\,I_f^*}{\frac{C_{fm}}{M_\infty}(F_\infty-I_f^*)}=\frac{((\gamma_f+\xi_f)F_\infty-C_{ff}(F_\infty-I_f^*))\,I_f^*M_\infty}{C_{fm}(F_\infty-I_f^*)F_\infty}, \quad (3.26)$$

and substituting this expression for I_m^* into the second equation of (3.25), we obtain the following equilibrium equation for I_f^*:

$$\left[M_\infty-\frac{((\gamma_f+\xi_f)F_\infty-C_{ff}(F_\infty-I_f^*))\,I_f^*M_\infty}{C_{fm}(F_\infty-I_f^*)F_\infty}\right]\cdot\left[\frac{C_{mf}}{F_\infty}I_f^*+\frac{((\gamma_f+\xi_f)F_\infty-C_{ff}(F_\infty-I_f^*))\,C_{mm}\,I_f^*}{C_{fm}(F_\infty-I_f^*)F_\infty}\right]$$

$$=(\gamma_m+\xi_m)\,\frac{((\gamma_f+\xi_f)F_\infty-C_{ff}(F_\infty-I_f^*))\,I_f^*M_\infty}{C_{fm}(F_\infty-I_f^*)F_\infty},$$

that is,

$$\left[F_\infty-\frac{((\gamma_f+\xi_f)F_\infty-C_{ff}(F_\infty-I_f^*))\,I_f^*}{C_{fm}(F_\infty-I_f^*)}\right]\cdot\left[C_{mf}I_f^*+\frac{((\gamma_f+\xi_f)F_\infty-C_{ff}(F_\infty-I_f^*))\,C_{mm}\,I_f^*}{C_{fm}(F_\infty-I_f^*)}\right]$$

$$=(\gamma_m+\xi_m)\,\frac{((\gamma_f+\xi_f)F_\infty-C_{ff}(F_\infty-I_f^*))\,I_f^*F_\infty}{C_{fm}(F_\infty-I_f^*)},$$

which is equivalent to

$$[F_\infty C_{fm}(F_\infty-I_f^*)-((\gamma_f+\xi_f)F_\infty-C_{ff}F_\infty+C_{ff}I_f^*))\,I_f^*]$$
$$\cdot\left[C_{mf}C_{fm}(F_\infty-I_f^*)+C_{mm}\,((\gamma_f+\xi_f)F_\infty-C_{ff}(F_\infty-I_f^*))\right]$$

$$= (\gamma_m + \xi_m)\,[(\gamma_f + \xi_f - C_{ff})F_\infty + C_{ff}I_f^*)]\,C_{fm}\,(F_\infty - I_f^*)\,F_\infty,$$

or

$$\Big[-C_{ff}\,(I_f^*)^2 + F_\infty[C_{ff} - C_{fm} - (\gamma_f + \xi_f)]\,I_f^* + C_{fm}\,(F_\infty)^2\Big]\cdot\Big[(C_{fm}C_{mf} - C_{ff}C_{mm})\,I_f^* + (C_{ff}C_{mm} - C_{fm}C_{mf})\,F_\infty - C_{mm}\,(\gamma_f + \xi_f)\,F_\infty\Big] = C_{ff}C_{fm}F_\infty(\gamma_m + \xi_m)(I_f^*)^2 + C_{fm}(\gamma_f + \xi_f - 2C_{ff})(F_\infty)^2(\gamma_m + \xi_m)\,I_f^* + C_{fm}(F_\infty)^3(\gamma_m + \xi_m)(C_{ff} - \gamma_f - \xi_f),$$

We see that the equilibrium values of I_f^* are the roots of the cubic polynomial

$$Ux^3 + Vx^2 + Wx + Z, \tag{3.27}$$

where,

$$\begin{aligned}
U &= C_{ff}\,\frac{C_{ff}C_{mm} - C_{fm}C_{mf}}{\bar{N}},\\
V &= C_{ff}[C_{mm}(\gamma_f + \xi_f) - C_{fm}(\gamma_m + \xi_m)] + \frac{C_{ff}C_{mm} - C_{fm}C_{mf}}{\bar{N}}\,[C_{fm}M_\infty + (\gamma_f + \xi_f)\bar{N} - 2\,C_{ff}F_\infty],\\
W &= 2\,C_{fm}F_\infty M_\infty\,\frac{C_{fm}C_{mf} - C_{ff}C_{mm}}{\bar{N}} + C_{fm}C_{mm}M_\infty\,(\gamma_f + \xi_f) - C_{fm}((\gamma_f + \xi_f)\bar{N} - 2C_{ff}F_\infty)\\
&\quad\times(\gamma_m + \xi_m) + [C_{ff}F_\infty - (\gamma_f + \xi_f)\bar{N}]\Big[\frac{C_{ff}C_{mm} - C_{fm}C_{mf}}{\bar{N}}\,F_\infty - C_{mm}\,(\gamma_f + \xi_f)\Big],\\
Z &= C_{fm}\,F_\infty\,M_\infty\Big[\frac{C_{ff}C_{mm} - C_{fm}C_{mf}}{\bar{N}}\,F_\infty - C_{mm}\,(\gamma_f + \xi_f)\Big] + C_{fm}F_\infty(\gamma_m + \xi_m)[(\gamma_f + \xi_f)\bar{N} - C_{ff}F_\infty]\\
&= C_{fm}\,F_\infty\,\bar{N}\Big[\mathcal{R}_0^f(\gamma_f + \xi_f)\mathcal{R}_0^m(\gamma_m + \xi_m) - \frac{C_{fm}C_{mf}}{\bar{N}^2}F_\infty M_\infty - \mathcal{R}_0^m(\gamma_m + \xi_m)(\gamma_f + \xi_f)\\
&\qquad + (\gamma_m + \xi_m)(\gamma_f + \xi_f)(1 - \mathcal{R}_0^f)\Big]\\
&= C_{fm}\,F_\infty\,\bar{N}\,(\gamma_f + \xi_f)\,(\gamma_m + \xi_m)\Big[(1 - \mathcal{R}_0^f)(1 - \mathcal{R}_0^m) - \frac{C_{fm}C_{mf}}{\bar{N}^2(\gamma_f + \xi_f)\,(\gamma_m + \xi_m)}F_\infty M_\infty\Big].
\end{aligned} \tag{3.28}$$

We can establish now sufficient conditions for a positive (endemic) equilibrium to exist.

Theorem 3.5. *Suppose that $C_{ff}C_{mm} > C_{fm}C_{mf}$. Then, if either $\mathcal{R}_0 > 1$ or $\mathcal{R}_0^f > 1$ and $\mathcal{R}_0^m > 1$, there exists (at least) one endemic equilibrium of* (2.6).

Proof. Being of odd degree, the polynomial (3.27) has (at least) one real root and the intermediate value theorem implies that $UZ < 0$ is a sufficient condition for it to have a positive root. We might then expect that the condition $UZ < 0$ should follow from (or, perhaps, be equivalent to) the threshold condition for the basic reproduction number, $\mathcal{R}_0 > 1$. However, in view of (3.21), $\mathcal{R}_0 > 1$ is equivalent to

$$C_{fm}C_{mf} > C_{ff}C_{mm}\left(1 - \frac{1}{\mathcal{R}_0^f}\right)\left(1 - \frac{1}{\mathcal{R}_0^m}\right). \tag{3.29}$$

For $\mathcal{R}_0 > 1$ (or $\mathcal{R}_0^f > 1$ and $\mathcal{R}_0^m > 1$), we see that (3.28) and (3.29) imply that

$$Z < C_{fm} F_\infty \bar{N} (\gamma_f + \xi_f)(\gamma_m + \xi_m) \left[(1 - \mathcal{R}_0^f)(1 - \mathcal{R}_0^m) - \frac{C_{ff} C_{mm} F_\infty M_\infty}{\bar{N}^2 (\gamma_f + \xi_f)(\gamma_m + \xi_m)} \left(1 - \frac{1}{\mathcal{R}_0^f}\right)\left(1 - \frac{1}{\mathcal{R}_0^m}\right) \right]$$
$$= C_{fm} F_\infty \bar{N} (\gamma_f + \xi_f)(\gamma_m + \xi_m) \left[(1 - \mathcal{R}_0^f)(1 - \mathcal{R}_0^m) - \mathcal{R}_0^f \mathcal{R}_0^m \left(1 - \frac{1}{\mathcal{R}_0^f}\right)\left(1 - \frac{1}{\mathcal{R}_0^m}\right) \right] = 0. \tag{3.30}$$

□

Note that, if we rewrite the first hypothesis, $C_{ff} C_{mm} > C_{fm} C_{mf}$, as

$$\frac{C_{ff}}{C_{fm}} \cdot \frac{C_{mm}}{C_{mf}} > 1,$$

we see that it could be interpreted as a condition on how same-sex transmission probabilities compare with opposite-sex transmission probabilities. For example, if we knew that transmission of infection from female to female is less likely than from female to male, the first ratio would actually be less than one, implying that the second ratio —which corresponds to males transmitting infection— would need to be sufficiently larger than one to compensate and make their product larger than one. This may well be the case for many STIs, but we can have scenarios where the opposite is true. For example, a population where same-sex partners are more risk adverse (i.e., use protection more frequently) than opposite-sex ones. This scenario is incompatible with the assumption above, suggesting that the first hypothesis in Theorem 3.5 may not be necessary for the existence and stability of an endemic equilibrium.

Sufficient conditions for uniqueness of the endemic equilibrium are $UZ < 0$ together with a condition for the other two roots of (3.27) to be complex conjugates, such as (see, e.g., [35])

$$\Delta = 18\, UVWZ - 4V^3 Z + V^2 W^2 - 4UW^3 - 27U^2 Z^2 < 0. \tag{3.31}$$

If $\Delta = 0$, then (3.27) has two distinct real roots (one simple and one double) and, if $\Delta > 0$, then (3.27) has three distinct real roots, but their signs could be any.

The condition $U > 0$ may be assumed without loss of generality because either the polynomial (3.27) or its opposite satisfy it (unless we have the singular case $C_{ff} C_{mm} = C_{fm} C_{mf}$) and Δ does not change if the polynomial is replaced by its additive inverse. However, if $C_{ff} C_{mm} < C_{fm} C_{mf}$, we would need to prove that $Z > 0$, which is incompatible with $\mathcal{R}_0 > 1$.

We were unable to prove the negativity of the discriminant Δ in (3.31) or the local asymptotic stability of endemic equilibria. Therefore, to have some numerical evidence for the former (which implies the existence of a unique endemic equilibrium) and for the latter (its local asymptotic stability) we used Latin Hypercube sampling to select one million random 6-tuples $(C_{ff}, C_{ff}, C_{ff}, C_{ff}, \gamma_f, \gamma_m)$ in the 6-dimensional hypercube $\mathcal{H}$ defined as the cross product of the allowable intervals of the positive real line for each of the six parameters

$$\mathcal{H} = [0.001, 10] \times [0.001, 10] \times [0.001, 10] \times [0.001, 10] \times [0.001, 5] \times [0.001, 5].$$

We kept Λ_f, Λ_m, ξ_f, and ξ_m fixed, as those were calculated directly from the data. Their values are estimated in [26]. For each of those 6-parameter combinations, we checked whether the conditions (3.31), $U > 0$, and $Z < 0$ were met. From those one million combinations, 296,646 met the conditions. We show in Figure 4 the curve $\mathcal{R}_0 = 1$ on the γ-plane together with color-coded dots in red and blue corresponding to the cases where the solutions approached the endemic or the disease-free equilibrium.

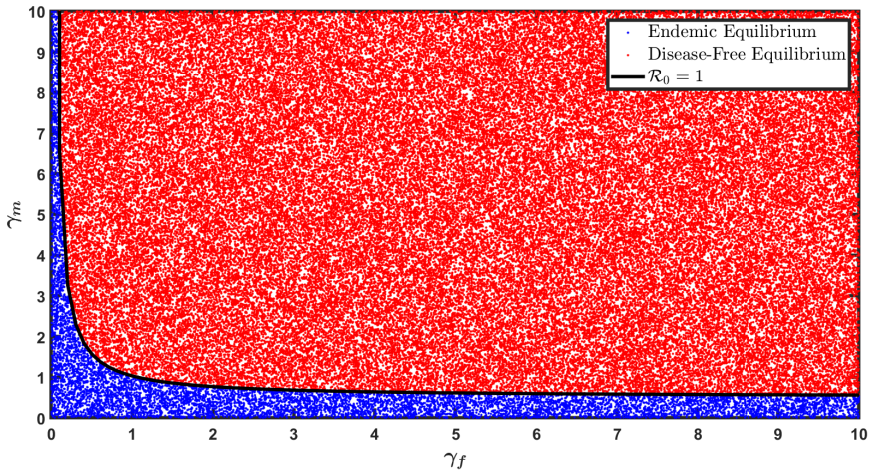

Figure 4. Equilibrium approached for many parameter combinations, showing just the values of γ_f and γ_m.

The numerical evidence above suggests that when a unique endemic equilibrium exists, it is globally asymptotically stable.

In Figure 5 below we show the example of parameter values $(\Lambda_f, \Lambda_m, \xi_f, \xi_m, \gamma_f, \gamma_m, C_{ff}, C_{fm}, C_{mm}, C_{mf}) = (3777794, 3872800, 0.196, 0.0238, 0.6868, 2.5807, 0.7249, 2.1900, 8.7674, 1.7700)$, which meet the conditions $U > 0$, $Z < 0$, and (3.31). These parameter values result in a cubic polynomial for I_f^* that has one real positive root $(93, 888, 455)$ and two complex conjugate roots, $P(x) = 5.06 \times 10^{-9}x^3 + 2.64x^2 + 1.95 \times 10^{-9}x - 2.10 \times 10^{17}$. Very different initial conditions were used for (a) and (b) to show that the model stabilizes at the equilibrium point $(S_f^*, S_m^*, I_f^*, I_m^*) = (98856112, 84911300, 93888455, 77811405)$ when the initial conditions are positive.

3.1.3. Parameter fitting

Figures 6 and 7 show the results of fitting model (2.6) to five years (2015-2019) of gonorrhea incidence data for females and males, respectively. The estimated parameter values, in conjunction with the initial conditions and the four fixed parameter values obtained in (2.12), are presented in Table 5. These results demonstrate that our model can capture the observed upward trend in gonorrhea incidence over the five-year period with rational and justifiable parameter values.

3.2. STI SIS model for dating app user results

We present analytical findings alongside parameter estimation results, which were obtained by fitting the model to ten years of incidence data. Additionally, we showcase the outcomes of both local

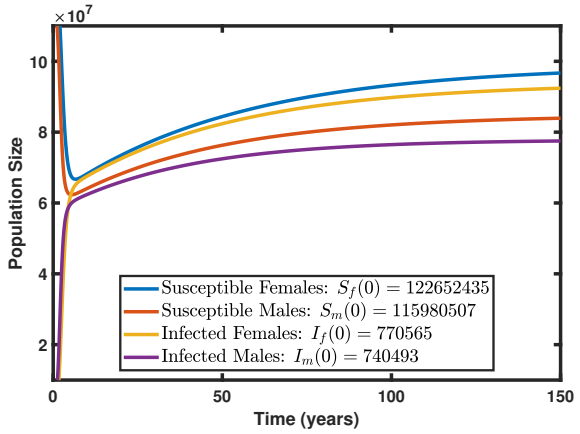

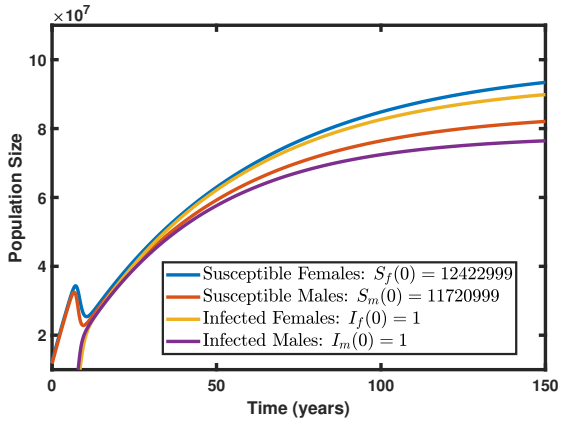

Figure 5. Example of time-series of the sizes of the four model compartments when there is a unique endemic equilibrium, corresponding to two different initial conditions.

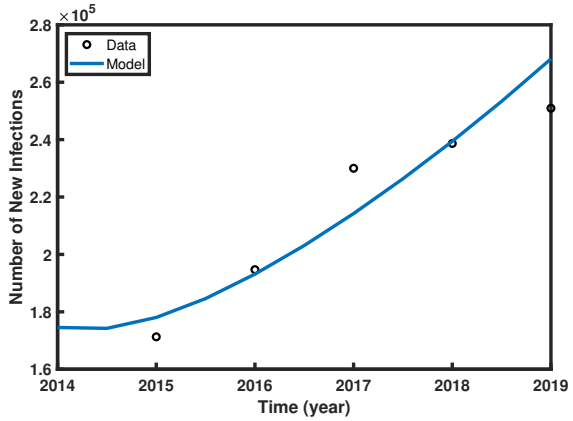

Figure 6. Fitting of simple SIS model to female gonorrhea incidence data.

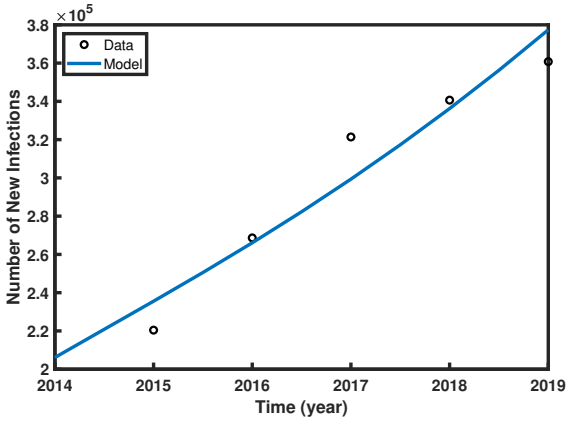

Figure 7. Fitting of simple SIS model to male gonorrhea incidence data.

Table 5. Initial values, fixed parameters, and fitted parameters of the simple SIS model to incidence data of gonorrhea.

Parameter	Fitted Value	Parameter	Fitted Value
$S_f(0)$	123,173,000	$S_m(0)$	116,460,000
$I_f(0)$	250,000	$I_m(0)$	261,000
Λ_f	3,777,793	Λ_m	3,872,800
ξ_f	0.020	ξ_m	0.024
γ_f	0.379	γ_m	0.817
C_{ff}	0.050	C_{mm}	0.729
C_{fm}	1.254	C_{mf}	0.947

and global sensitivity analyses, as well as various scenario analyses.

3.2.1. The invariant cone in the positive orthant

We show that the non-negative orthant of $\mathbb{R}^8$ is invariant under the flow of system (2.27)–(2.34). This is done in an entirely analogous way as done for the simple model, Theorem 3.1.

Theorem 3.6. *The cone*

$$\left\{\left(S_f^n, S_f^u, S_m^n, S_m^u, I_f^n, I_f^u, I_m^n, I_m^u\right) \in \mathbb{R}^8 : S_f^n + S_f^u + S_m^n + S_m^u + I_f^n + I_f^u, + I_m^n + I_m^u \leq \frac{\Lambda}{\mu}\right\}$$

is invariant under the flow of system (2.27)–(2.34).

Proof. Starting with the equations for the four compartments of susceptible individuals, equations (2.27), (2.29), (2.31), and (2.33), we write equivalent ones (which are just (3.4) with the parameters now distinguishing app-user status)

$$\frac{d}{dt}\left(S_g^s e^{\xi_g t + \int_0^t \lambda_g^s(\tau)d\tau}\right) = \left[\Lambda_g^s + \gamma_g^s I_g^s(t)\right] e^{\xi_g t + \int_0^t \lambda_g^s(\tau)d\tau} > 0, \qquad g \in \{f, m\}, \quad s \in \{n, u\},$$

whereby

$$S_g^s(t) e^{\xi_g t + \int_0^t \lambda_g^s(\tau)d\tau} - S_g^s(0) = \Lambda_g^s \int_0^t e^{\xi_g v + \int_0^v \lambda_g^s(\tau)d\tau} dv + \gamma_g^s \int_0^t I_g^s(v)\, e^{\xi_g v + \int_0^v \lambda_g^s(\tau)d\tau} dv.$$

Hence, for $g \in \{f, m\}$, $s \in \{n, u\}$, and as long as the infected class sizes stay positive,

$$S_g^s(t) = S_g^s(0)\, e^{-\xi_g t - \int_0^t \lambda_g^s(\tau)d\tau} + \int_0^t \left[\Lambda_g^s + \gamma_g^s I_g^s(v)\right] e^{-\xi_g(t-v) - \int_v^t \lambda_g^s(\tau)d\tau} dv > 0. \tag{3.32}$$

Concerning the four compartments of infected individuals, we note that (2.24)–(2.26) imply that at least one of the four compartments of infected is non-empty, say I_f^N; this makes the two forces of infection $\lambda_f^n > 0$ and $\lambda_f^u > 0$, whereby, by continuity of solutions, for $t > 0$ small enough, necessarily $I_f^n(t) > 0$, $I_m^n(t) > 0$, and $I_M^u(t) > 0$. Hence, $\lambda_f^u(t) > 0$ for $t > 0$ small enough and, even if $\lambda_f^u(0) = 0$, (2.32) leads to $I_f^u(t) > 0$ for $t > 0$ small enough.

Also, equations (2.28), (2.30), (2.32), and (2.34) imply that, as long as the sizes of the susceptible classes are positive,

$$I_g^s(t) = I_g^s(0)\, e^{-\xi_g t - \int_0^t \lambda_g^s(\tau)d\tau} + \int_0^t \lambda_g^s(v)\, S_g^s(v)\, e^{-\xi_g(t-v) - \int_v^t \lambda_g^s(\tau)d\tau} dv > 0. \tag{3.33}$$

In summary, for $t > 0$ small enough, $S_g^s(t) > 0$ and $I_g^s(t) > 0$ for all four combinations of sex and dating-app-user status. We want to show that the positivity stays true *for all* time $t > 0$.

Suppose that this is not the case, and consider the smallest positive time $\bar{t}$ at which one of these eight compartments of susceptible or infected individuals is empty,

$$\bar{t} = \min\{t > 0 : S_f^n(t) \cdot S_f^u(t) \cdot S_m^n(t) \cdot S_m^u(t) \cdot I_f^n(t) \cdot I_f^u(t) \cdot I_m^n(t) \cdot I_m^u(t) = 0\}. \tag{3.34}$$

It follows that, for $t \in (0, \bar{t})$, $S_f^n(t), S_f^u(t), S_m^n(t), S_m^u(t) > 0$, $I_f^n(t), I_f^u(t), I_m^n(t), I_m^u(t) > 0$ and *a fortiori*, because of (2.24), we have all four forces of infection positive on that interval: $\lambda_f^n(t)$, $\lambda_f^u(t)$, $\lambda_m^n(t)$, $\lambda_m^u(t) > 0$ for $t \in (0, \bar{t})$. Consequently, because of (3.32) and (3.33), we have

$$S_f^n(\bar{t}), S_f^u(\bar{t}), S_m^n(\bar{t}), S_m^u(\bar{t}) > 0, I_f^n(\bar{t}), I_f^u(\bar{t}), I_m^n(\bar{t}), I_m^u(\bar{t}) > 0,$$

contradicting (3.34). Hence, such time does not exist. The upper bound now follows from the solutions to the equations for $F^s = S_f^s + I_f^s$ and $M^s S_m^s + I_m^s$, $s = f, m$ derived exactly as (2.9) and (2.10) are from (2.7) and (2.8). □

3.2.2. Simulations: STI incidence on the rise

Figures 8 and 9 show the estimated percent increase during the previous 12 months in female and male STI incidence and prevalence, respectively, attributable to dating apps use that occurred between 2015 and 2019. We estimated the percentages attributable to dating apps use by comparing model output corresponding to the per capita contact rates differentiated for dating apps users and non-users with output corresponding to the rates for users being set at the (lower) values of non-users. We see that, for prevalence, those percentages are between 10%–20%, suggesting that more research designed to better understand the relationship between STIs and dating apps is a worthwhile endeavor.

Regarding female prevalence, for example, Figure 9 shows that from 2018 to 2019 there was an 8.7% increase attributable to dating apps. In a similar fashion, this figure shows a 9.2% increase in male prevalence due to dating apps between 2018 and 2019, with the annual percentage of change stabilizing at around 8-9% with increasing time.

Consistent with the trends discussed above, Figure 8 referring to the annual percentage of change in female and male incidence over time display their trend-lines stabilizing at 9.9% and 6%, respectively. As all figures indicate the stabilization of the annual percentage of change in STIs is a positive value, it is suggested that both the incidence and prevalence of STIs are continuing to rise over time. This information provides additional motivation for the inquiry into the quantifiable effects of dating app usage on the proliferation of STIs.

The parameter names and their fitted values are shown in Table 6, while the graphs of the model output together with the incidence data appear in Figures 10 and 11. The fitting in Figure 10 is not very good because the female incidence data for chlamydia and gonorrhea for 2009 is unusually high and our model uses it as the initial value for the following years' predictions.

3.2.3. Sensitivity Analysis

We performed sensitivity analyses of incidence and prevalence by sex for four γ_g^s parameters and eight $C_{g_1 g_2}^{s_1 s_2}$ parameters. We found that γ_m^u and γ_f^u have the greatest impact on the prevalence and incidence of the STIs in our study (for chlamydia and gonorrhea). This finding is consistent with the literature, as users of dating apps are shown to engage in more risky behaviors that are linked to STI transmission. The corresponding sensitivity curves are shown below, where the baseline values correspond to the fitted ones shown in Table 6.

The sensitivity curve for γ_f^u, Figure 12, shows that a 1% increase in γ_f^u results in a 2.65% decrease

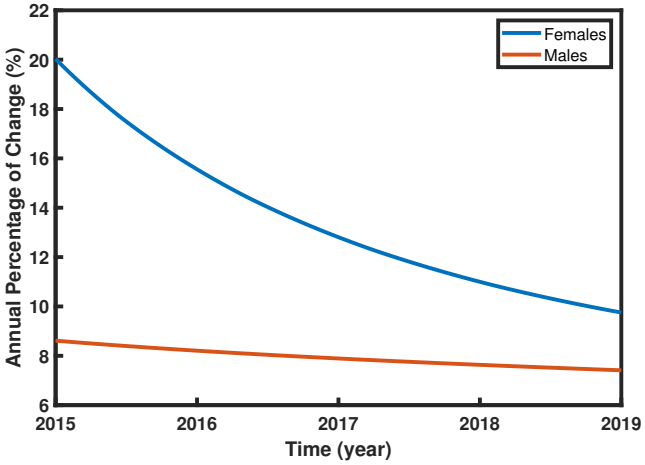

Figure 8. Annual increase in incidence due to dating apps.

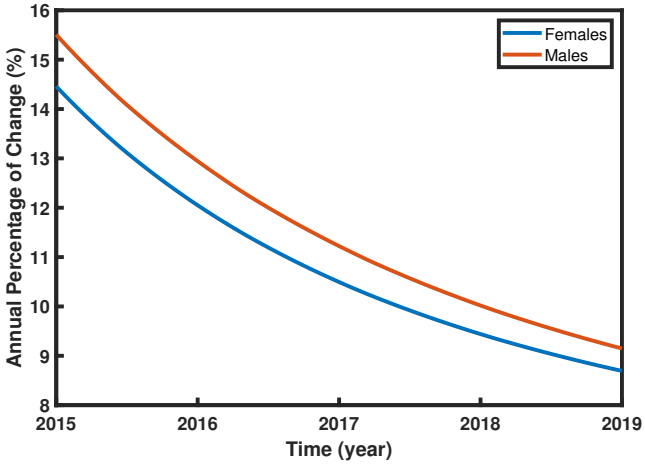

Figure 9. Annual increase in prevalence due to dating apps.

Table 6. Parameters estimated by fitting the model to incidence data.

Parameter	Fitted Value
γ_f^n	1.868
γ_f^u	0.779
γ_m^n	0.615
γ_m^u	1.132
C_{mf}^{nn}	0.709
C_{mf}^{un}	0.942
C_{mf}^{nu}	0.100
C_{mf}^{uu}	5.770
C_{fm}^{nn}	5.722
C_{fm}^{un}	0.346
C_{fm}^{nu}	1.586
C_{fm}^{uu}	7.777

in female prevalence and a 2.45% decrease in male prevalence. In contrast, based on Figure 13, a 1% increase in γ_m^u results in a 3.4% decrease in male prevalence and a 3.1% decrease in female prevalence.

In addition, a comparison of the sensitivity curves at the baseline values for γ_f^u and γ_m^u, indicates that the population of male users presents the most obvious gender/behavior group to target for prevention measures from the perspective of cost-benefit of such public health interventions. A 1% change in the parameter value *in either direction* would have a significant impact on the corresponding STI prevalence.

Similarly, the sensitivity curves of $C_{g_1g_2}^{s_1,s_2}$ suggest that C_{mf}^{uu} and C_{fm}^{uu} have the greatest impact on the prevalence and incidence of STIs. This finding is consistent with our intuition because increased sexual risk behavior is associated with dating app users and, as such, C_{mf}^{uu} and C_{fm}^{uu} are expected to have a larger impact on the prevalence and incidence of STIs. The corresponding sensitivity curves are shown in Figures 14 and 15. These figures indicate that a 1% increase (respectively, decrease) in C_{mf}^{uu}

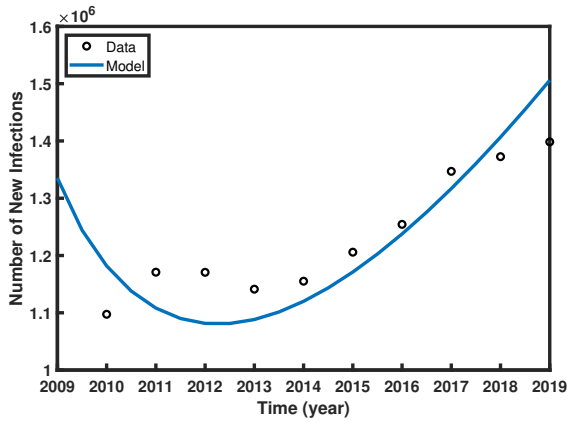

Figure 10. Female incidence chlamydia and gonorrhea.

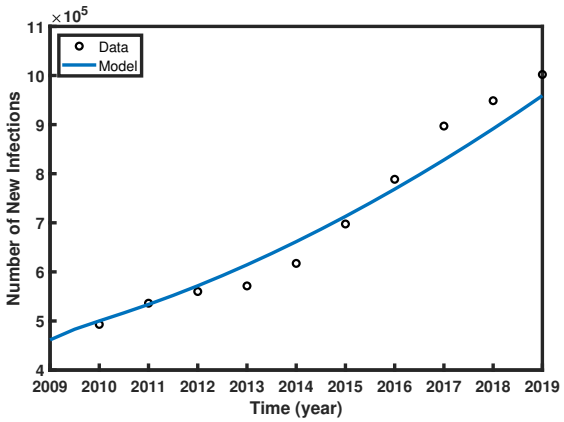

Figure 11. Male incidence chlamydia and gonorrhea

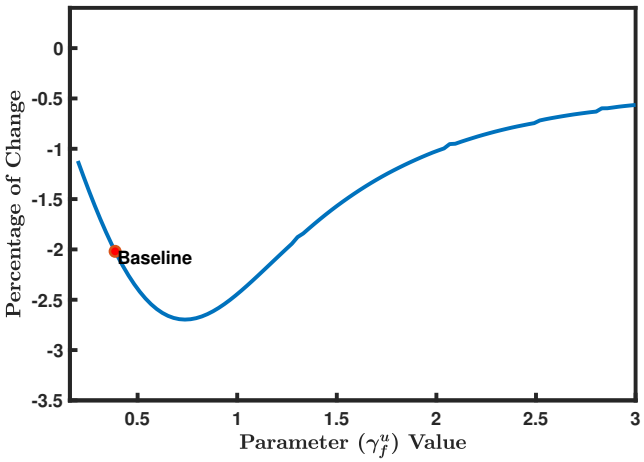

Figure 12. Sensitivity of γ_f^u on female prevalence.

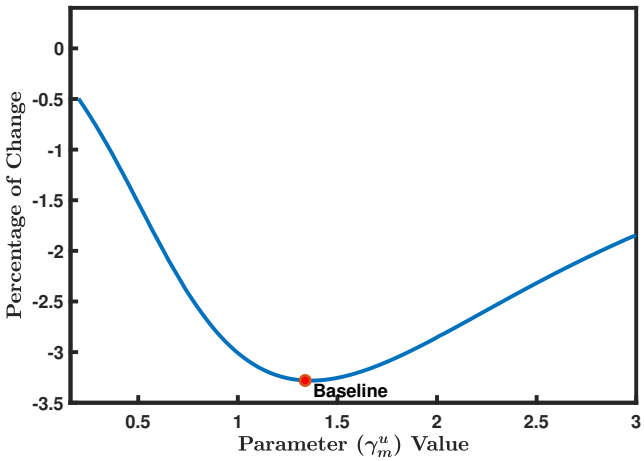

Figure 13. Sensitivity of γ_m^u on male prevalence

from its baseline value would results in a 2.6% increase (respectively, decrease) in male prevalence, whereas a 1% increase in C_{fm}^{uu} results in a 2.7% increase in female prevalence. Also, the companion curves not shown here suggest that a 1% increase in C_{mf}^{uu} would result in a 2.2% increase in female prevalence while a 1% increase in C_{fm}^{uu} would lead to a 2.5% increase in male prevalence.

Careful examination of the sensitivity curves of prevalence and incidence for γ_g^s and $C_{g_1g_2}^{s_1s_2}$ reveals that perturbations among the male dating app users results in consistently greater percent changes in the incidence and prevalence of STIs, in comparison to the other sex/behavior classes. From a public health standpoint, this presents male dating apps users as the most impactful sex/behavior population for an intervention.

3.2.4. Global Sensitivity: Partial Rank Correlation Analysis (PRCA)

We performed Partial Rank Correlation Analysis (PRCA) for the 12 fitted model parameters, γ_g^s and $C_{g_1g_2}^{s_1s_2}$, and for the four pertinent sex/behavior populations. The resulting Partial Rank Correlation

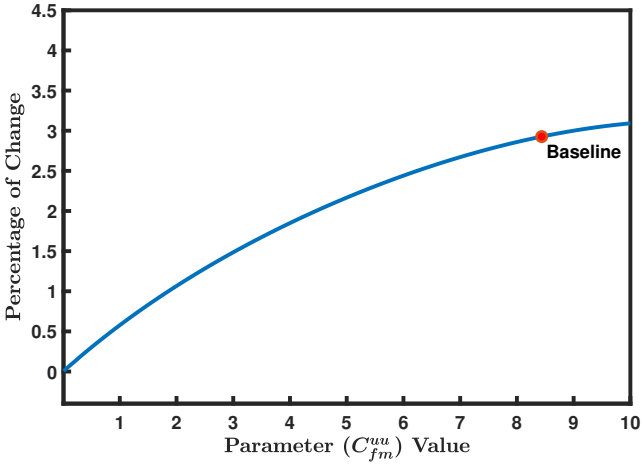

Figure 14. Sensitivity of C^{uu}_{fm} on female prevalence.

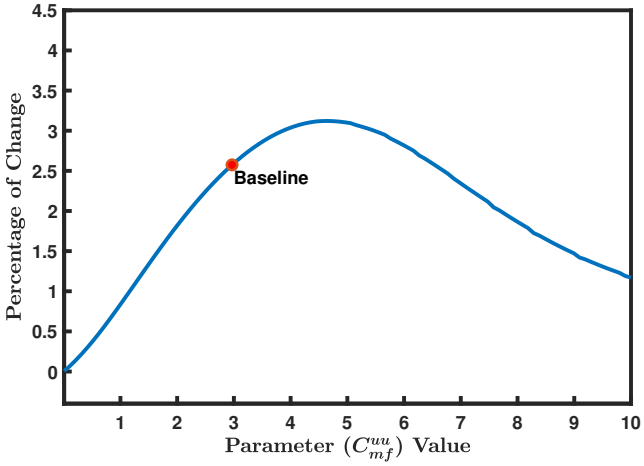

Figure 15. Sensitivity of C^{uu}_{mf} on male prevalence.

Coefficients (PRCC) for the former are shown in Figure 16.

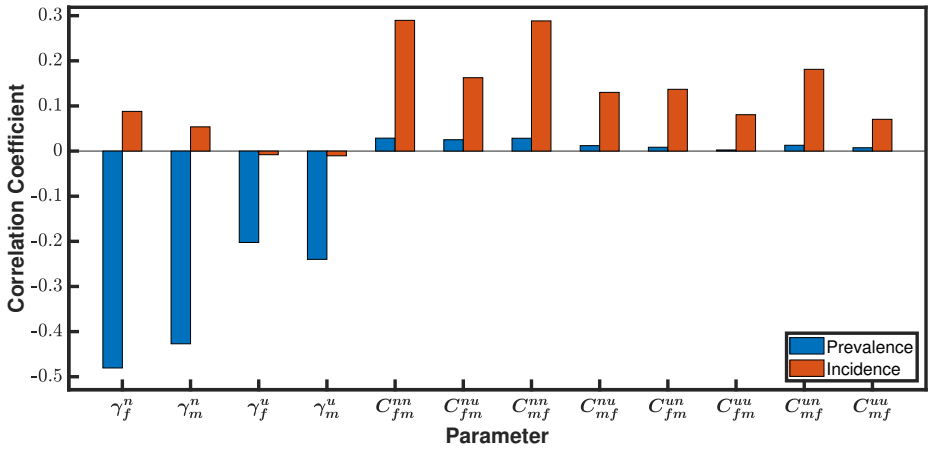

Figure 16. PCRA of Fitted Parameters.

The signs of the correlation coefficients for γ^s_g differ for incidence and prevalence, with the ones for prevalence being negative. These negative correlations agree with the intuition that larger γ^s_g corresponds to a smaller duration of infection and, consequently, to reduced prevalence. In contrast, the PRCCs for γ^s_g and incidence are positive, both for females and males. This is likely due to the fact that larger values of γ^s_g correspond to a larger susceptible class, and incidence is represented in the model by $\lambda(I(t))S(t)$, where, despite λ being smaller for larger γ^s_g, its product with S can still become larger.

Contrasting with what we observe for γ^s_g, the PRCCs for all combinations of $C^{s_1s_2}_{g_1g_2}$ and incidence and prevalence are positive. This suggests that, as the unit per capita transmission rate from sex g_2 to sex g_1 assumes larger values, there will be both greater incidence and prevalence of STIs. This conclusion is aligned with our intuitive expectation.

Figure 17 displays the partial rank correlation coefficients for the eight combinations between the four pertinent sex/behavior populations and the incidence and prevalence of STIs. Looking at the

PRCCs for STI incidence, we see that the ones corresponding to both female and male dating app users are positive, while those for non-users are negative. This observation strongly suggests that dating app users have a greater responsibility than non-users for the increased incidence of STIs. This is supported by further analysis of the correlation coefficients for male dating app users and non-users. For instance, for STI incidence, male users (r = 0.9) maintain a strong positive correlation, and male nonusers a strong negative correlation (r = -0.9). Moreover, sex comparisons among dating app users and non-users show males as having a greater relationship with STI incidence than females from either population. From a public health standpoint, this argues for male dating apps users being the best target population for intervention strategies.

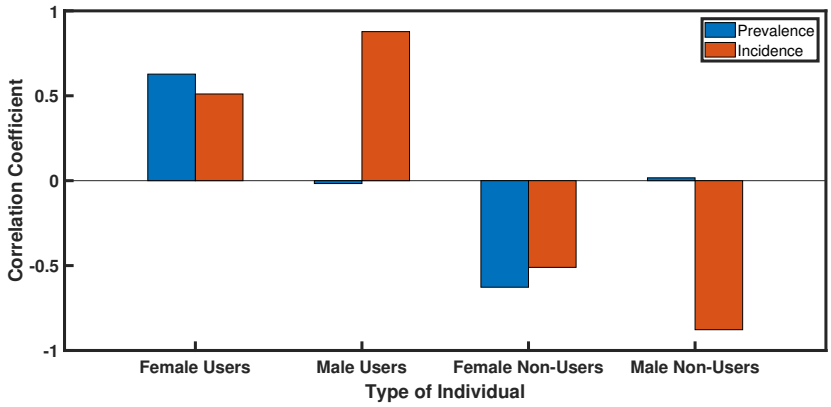

Figure 17. PCRA of Sex/Behavior Categories.

Figure 17 also provides assessments for STI prevalence and incidence as they relate to the four previously mentioned sex/behavior categories. For female dating app users and non-users, the moderately strong correlation coefficients (r = 0.6 and -0.6, respectively) are quite intuitive: STI prevalence and incidence increase as the number of female users increases, and decreases as the number of female non-users increases. In contrast, the partial rank correlation coefficients for STI prevalence among male dating app users and non-users are very different from those for females, as they are both very close to zero and, thus, indicate no apparent significant correlation between dating app use by males and STI prevalence.

3.2.5. Scenario Analysis

Various scenario analyses were conducted to assess the potential impact of ad campaigns being implemented into dating apps to reduce risky sexual behaviors, such as reduced condom usage or increased numbers of sexual partners. The results obtained indicate that a reduction in the per capita infectivity from male to female dating app users has a significant impact on reducing prevalence and incidence for both sexes. The greatest reduction is in female incidence, where the percentage reduction is approximately twice the reduction in male prevalence (see Table 7). The results for that scenario for male incidence are presented as an example in Figure 18.

Table 7 presents the summary of the large potential impact after two years resulting from the scenario analysis described above, as the percentage change in STI incidence and prevalence due to 10%, 20%, 30%, and 40% reductions in C_{fm}^{uu}.

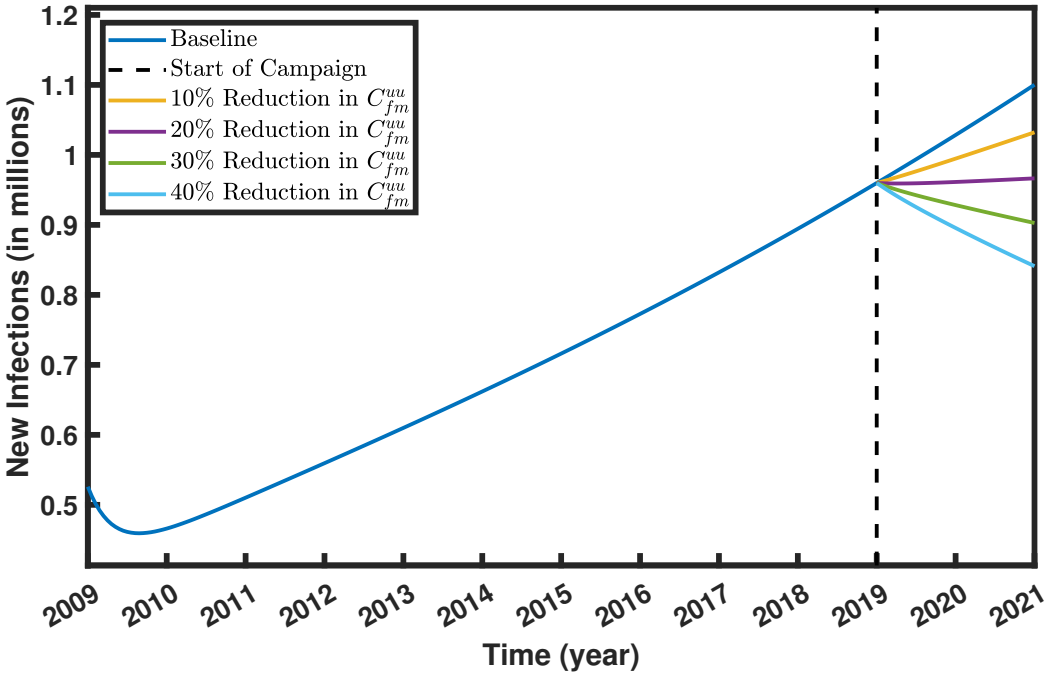

Figure 18. C_{fm}^{uu} Scenario Analysis: Potential Impact of Pop-Up Ads on Male Incidence.

Table 7. C_{fm}^{uu} scenario analysis results.

% Reduction in C_{fm}^{uu}	Male Prevalence	Male Incidence	Female Prevalence	Female Incidence
10	4.2	7.3	4.9	7.6
20	7.3	10.9	11.3	15.9
30	11.2	18.2	18.7	23.5
40	14.6	23.6	21.7	29.4

The corresponding scenario analysis results for reductions of 10%–40% in per capita transmissibility rates from female to male sexual partners, both being dating app users, C_{mf}^{uu}, are displayed in the Table 8 below.

Table 8. C_{mf}^{uu} scenario analysis results.

% Reduction in C_{mf}^{uu}	Male Prevalence	Male Incidence	Female Prevalence	Female Incidence
10	4.5	13.6	7.1	7.6
20	12.6	22.7	9.5	14.7
30	22.9	34.5	15.7	22.4
40	28.7	40.9	19.0	29.4

We can see in Table 8 that a 40% reduction in C_{mf}^{uu} would result in a 40.9% decrease in male incidence and a 29.4% decrease in female incidence. This projected reduction in male incidence is almost twice that corresponding to a 40% reduction in C_{fm}^{uu} (Table 7), as is the projected reduction in male prevalence (14.6% in Table 7 compared with 28.7% in Table 8). Perhaps more importantly, for a small

reduction of 10% in C^{uu}_{mf}, we see a much larger projected impact on male incidence from reducing female-to-male transmission than from male-to-female (7.3% in Table 7 compared with 13.6% in Table 8), with a similar advantage concerning female prevalence (4.9% in Table 7 compared with 7.1% in Table 8).

The analogous scenario analyses for 10%–40% increases in γ^u_f and γ^u_m show quite smaller impact on STI prevalence and incidence than the same percentage increase in C^{uu}_{mf} or C^{uu}_{fm}. They also show that reductions of γ^u_m result in a much greater decrease in female incidence and male prevalence than analogous reductions in γ^u_f. This suggests that campaigns targeted at reducing the mean infectious time of male dating apps users (e.g., by getting tested and seeking treatment as soon as possible) have good potential for reducing STI incidence and prevalence.

These findings suggest that pop-up ads or other related public health campaigns targeting dating apps users, particularly males, may potentially be very helpful in reducing STI incidence and prevalence.

4. Conclusions

This study utilized mathematical modeling and statistical analysis to first create a model of the age and sex structure of the sexually active population of the U.S. in order to pursue the main goal of investigating the relationship between dating app usage and STI incidence and prevalence. A four-compartment SIS STI model and an eight-compartment SIS STI model were created based on data collected from various sources, most prominently the CDC and WHO. In conjunction, these models were used to quantify the impact of dating apps on STI incidence rates. An equation decomposing the mean duration of infection was used to estimate the percentage of people who seek treatment after being diagnosed with an STI. Additionally, a modified version of the eight-compartment model allowed us to assess the potential impact of in-app prevention campaigns.

The four-compartment two-sex SIS STI model was constructed primarily to guide the choice of the parameters used in the eight-compartment two-sex dating-app SIS STI model. The model was also used to study the variability of fit with respect to simulation period and particular STIs or combinations of them, as well as to assess the correspondence between the model output and the incidence data. This is the first model that explicitly incorporates infection spread through the four combinations of sexes (FF, FM, MF, and MM).

For the four-compartment model, we first provided a method to estimate the sexually active population by sex and age, and then fitted the model (demographic) parameters to data, thus estimating the recruitment rates by sex, Λ_g, and the per capita exit rates by sex, ξ_g. Those values were then used in the model to estimate the remaining 6 (epidemiological) parameters, γ_f, γ_m, C_{fm}, C_{mm}, C_{mf}, and C_{ff}, by fitting model predictions to available data for STI incidence by sex. For the parameter fitting we utilized a MATLAB routine based on a descent method.

For our eight-compartment two-sex dating-app STI SIS model, we only considered opposite-sex sexual contacts for two main reasons. First, there are important gaps in available data regarding same-sex sexual partners by dating app usage. Second, considering transmission across all combinations of sexes and dating app usage status would require the use of an additional 8 constants in the forces of

infection λ_g, leading to a significant loss of validity in the parameter identification. Also, the extant literature suggests that the proportion of same-sex sexual contacts among all sexual contacts is small. Hence, we are assuming that disregarding same-sex sexual contacts will only have a small effect on the study's findings concerning overall incidence and prevalence.

The eight-compartment model was used to conduct a series of simulations designed to address our research goals: to quantify the percentage change in STI incidence and prevalence that results from dating app usage, to assess the potential impact of pop-up ads on the incidence and prevalence of STIs, and to identify the most important sex/behavior group to target for public-health interventions. From our simulations we concluded that both STI incidence and prevalence for females and males have increased annually by 9%–15% between 2015 and 2019 due to dating app usage, and that STI incidence and prevalence will continue to increase in the future.

Sensitivity analysis for γ_g and $C_{g_1g_2}^{s_1s_2}$ provided some useful information regarding the most influential sex/behavior population to target for public health interventions. We found that $C_{f_m}^{uu}$ and $C_{m_f}^{uu}$ correspond with the largest percentage changes in the prevalence and incidence of STIs. As such, users of dating apps are likely to have more impact on the rising STI rates in the United States than non-users. This claim is further supported by the sensitivity analysis for γ_g as incidence and prevalence of STIs are more sensitive to γ_f^u and γ_m^u than to γ_f^n and γ_m^n, with γ_m^u having the greatest impact on male and female prevalence. In summary, it can be stated with reasonable confidence that male dating app users are likely the optimal sex/behavior group to target for a public health intervention.

Global sensitivity analysis using the PRCC for γ_g^s and $C_{g_1g_2}^{s_1s_2}$ and for the four pertinent sex/behavior populations, confirms male users as the optimal target group for in-app prevention campaigns. We found that the PRCC for male dating app users and STI incidence has the largest positive magnitude, while the PRCC for male dating app non-users and STI incidence has the largest negative magnitude. These statistics further indicate male users as the sex/behavior group of interest with regard to a public health intervention campaign.

Concerning public health interventions, our scenario analyses for γ_g^s and $C_{g_1g_2}^{s_1s_2}$ indicate that reductions in C_{mf}^{uu} and/or in C_{fm}^{uu} may lead to important reductions of STI incidence and prevalence. This suggests that in-app prevention campaigns may provide a valuable strategy to control the rise in prevalence and incidence of STIs. More specifically, our results from scenario analyses, sensitivity analyses, and a PRCC study suggest that male dating app users are likely the most impactful group to target for prevention campaigns.

Some important limitations in this study were the lack of compatible data the models require, particularly for STI prevalence necessary to define initial conditions for the models. Sources contain abundant data on incidence, but are very scant on prevalence of STIs. In fact, a bonus of these models is that they provide estimates for prevalence that may be useful when real-life data is unavailable or non-existent. Similarly, we had to combine data from different points in time and/or different STIs, because the data needed for our models was usually not available with the necessary detail or completeness.

Use of AI tools declaration

The authors declare they have not used Artificial Intelligence (AI) tools in the creation of this article.

Acknowledgments

The authors thank the National Science Foundation for award DMS #2150492, and the Office of the Dean of The College of Liberal Arts and Sciences at Arizona State University for funding this research.

Conflict of interest

The authors declare there is no conflict of interest.

References

1. Centers for Disease Control and Prevention, Incidence, Prevalence, and Cost of Sexually Transmitted Infections in the United States, *Fact Sheets*, 2022. Available from: https://www.cdc.gov/nchhstp/newsroom/fact-sheets/std/STI-Incidence-Prevalence-Cost-Factsheet.htm
2. World Health Organization, Sexually transmitted infections (STIs), *Fact Sheets*, 2022. Available from: https://www.who.int/news-room/fact-sheets/detail/sexually-transmitted-infections-(stis)
3. T. Morris, Dating in 2021: Swiping left on COVID-19, *Global Web Index*, 2021. Available from: https://blog.gwi.com/chart-of-the-week/online-dating/
4. M. Lenahan, Dating app engagement surpasses pre-pandemic levels, *Apptopia*, 2020. Available from: https://blog.apptopia.com/dating-app-engagement-has-surpassed-pre-pandemic-levels
5. S. Dixon, U.S. smartphone dating app users 2019–2023, *Statista*, 2022. Available from: https://www.statista.com/statistics/274144/smartphone-dating-app-users-usa/
6. R. A. Bable, J. Ackerlund Brandt, Delay Discounting, Dating Applications, and Risky Sexual Behavior: An Exploratory Study, *Psychol. Record*, **72** (2022), 1–6. https://doi.org/10.1007/s40732-021-00506-6
7. A. N. Sawyer, E. R. Smith, E. G. Benotsch, Dating application use and sexual risk behavior among young adults, *Sexual. Res. Soc. Policy*, **15** (2018), 183–191. https://doi.org/10.1007/s13178-017-0297-6
8. Centers for Disease Control and Prevention, Sexually Transmitted Disease Surveillance, 2021. Available from: https://www.cdc.gov/std/statistics/2021/tables/5a.htm
9. Centers for Disease Control and Prevention, The State of STDs – Infographic. Available from: https://www.cdc.gov/std/statistics/infographic.htm

10. J. M. Kesten, K. Dias, F. Burns, P. Crook, A. Howarth, C. H. Mercer, et al., Acceptability and potential impact of delivering sexual health promotion information through social media and dating apps to MSM in England: A qualitative study, *BMC Public Health*, **19** (2019), 1–9. https://doi.org/10.1186/s12889-019-7558-7

11. A. Lajmanovich, J. A. Yorke, A deterministic model for gonorrhea in a nonhomogeneous population, *Math. Biosci.*, **28** (1976), 221–236. https://doi.org/10.1016/0025-5564(76)90125-5

12. H. W. Hethcote, J. A. Yorke, Gonorrhea Transmission Dynamics and Control, in *Lecture Notes in Biomathematics*, Vol. 56, Springer-Verlag, (1984), Berlin and New York. https://doi.org/10.1007/978-3-662-07544-9

13. K. Dietz, K. P. Hadeler, Epidemiological models for sexually transmitted diseases, *Journal of mathematical biology*, **26** (1988), 1–25. https://doi.org/10.1007/BF00280169

14. M. E. Kretzschmar, Deterministic and stochastic pair formation models for the spread of sexually transmitted diseases, *J. Biol. Syst.*, **3** (1995), 789–801. https://doi.org/10.1142/S0218339095000721

15. M. E. Kretzschmar, Y. T. van Duynhoven, A. J. Severijnen, Modeling prevention strategies for gonorrhea and chlamydia using stochastic network simulations, *American Journal of Epidemiology*, **144** (1996), 306–317. https://doi.org/10.1093/oxfordjournals.aje.a008926

16. M. E. Kretzschmar, R. Welte, A. van den Hoek, M. J. Postma, Comparative model-based analysis of screening programs for chlamydia trachomatis infections, *Am. J. Epidemiol.*, **153** (2001), 90–101. https://doi.org/10.1093/aje/153.1.90

17. M. E. Kretzschmar, K. M. E. Turner, P. M. Barton, W. J. Edmunds, N. Low, Predicting the population impact of chlamydia screening programmes: Comparative mathematical modelling study, *Sexual. Transmit. Infect.*, **85** (2009), 359–366. https://doi.org/10.1136/sti.2009.036251

18. M. Kretzschmar, J. C. M. Heijne, Pair formation models for sexually transmitted infections: A primer, *Infect. Disease Model.*, **2** (2017), 368–378. https://doi.org/10.1016/j.idm.2017.07.002

19. W. M. Geringer, M. Hinton, Three models to promote syphilis screening and treatment in a high risk population, *J. Commun. Health*, **18** (1993), https://doi.org/10.1007/BF01325158

20. F. A. Milner, R. Zhao, A new mathematical model of syphilis, *Math. Model. Nat. Phenom.*, **5** (2010), 96–108.

21. P. L. Peterson, D. G. Ostrow, D. J. McKirnan, Behavioral interventions for the primary prevention of HIV infection among homosexual and bisexual men, *J. Primary Prevent.*, **12** (1991), 19–34. https://doi.org/10.1007/BF01326539

22. O. Angulo, F. A. Milner, L. Sega, A SIR epidemic model structured by immunological variables, *J. Biol. Syst.*, **21** (2013). https://doi.org/10.1142/S0218339013400135

23. O. Angulo, F. A. Milner, L. Sega, Immunological models of epidemics, *MACI (Matemática Aplicada, Computacional e Industrial)*, **4** (2013), 53–56.

24. G. R. Bauer, S. L. Welles, Beyond assumptions of negligible risk: sexually transmitted diseases and women who have sex with women, *Am. J. Public Health*, **91** (2001), 1282–1286. https://doi.org/10.2105/ajph.91.8.1282

25. E. Torrone, J. Papp, H. Weinstock, Prevalence of Chlamydia trachomatis Genital Infection Among Persons Aged 14–39 Years — United States, 2007–2012, *Morbid. Mortal. Weekly Rep.*, **63** (2014), 834–838.

26. C. Bustamante Orellana, J. Lyerla, A. Martin, F. Milner, E. Smith, Estimating the structure by age and sex of the US sexually active population, *Math. Popul. Stud.*, Routledge, (2024). https://doi.org/10.1080/08898480.2024.2301868

27. B. G. Everett, Sexual orientation disparities in sexually transmitted infections: examining the intersection between sexual identity and sexual behavior, *Arch. Sexual Behav.*, **42** (2013), 225–236. https://doi.org/10.1007/s10508-012-9902-1

28. P. A. Cavazos-Rehg, M. J. Krauss, E. L. Spitznagel, M. Schootman, K. K. Bucholz, J. F. Peipert, et al., Age of sexual debut among US adolescents, *Contraception*, **80** (2009), 158–162. https://doi.org/10.1016/j.contraception.2009.02.014

29. C. L. Althaus, K. M. Turner, B. V. Schmid, J. C. Heijne, M. Kretzschmar, N. Low, Transmission of Chlamydia trachomatis through sexual partnerships: A comparison between three individual-based models and empirical data, *J. Royal Soc. Int.*, **9** (2021), 136–146. https://doi.org/10.1098/rsif.2011.0131

30. R. D. Kirkcaldy, E. Weston, A. C. Segurado, G. Hughes, Epidemiology of gonorrhoea: A global perspective, *Sex Health*, **16** (2019), 401–411. https://doi.org/10.1071/SH19061

31. E. Arias, M. Heron, J. Xu, United States Life Tables, 2014, *Nat. Vital Stat. Rep.*, **66** (2017), Division of Vital Statistics.

32. M. Iannelli, A. Pugliese, *An introduction to mathematical population dynamics*, Springer Cham, (2014). https://doi.org/10.1007/978-3-319-03026-5

33. C. Vargas de León, On the global stability of SIS, SIR and SIRS epidemic models with standard incidence, *Chaos Solit. Fract.*, **44** (2011), 1106–1110. https://doi.org/10.1016/j.chaos.2011.09.002

34. P. van den Driessche, J. Watmough, Reproduction numbers and sub-threshold endemic equilibria for compartmental models of disease transmission, *Math. Biosci.*, **180** (2002), 29—48. https://doi.org/10.1016/s0025-5564(02)00108-6

35. A. E. Ontiveros Salazar, P. H. Goh, S. Kasliwal, J. Khim, Cubic Discriminant, *Brilliant.org*. Available from: `https://brilliant.org/wiki/cubic-discriminant/`

AIMS Press